Organic & Biomolecular Chemistry

www.rsc.org/obc

Volume 10 | Number 18 | 14 May 2012 | Pages 3565–3768

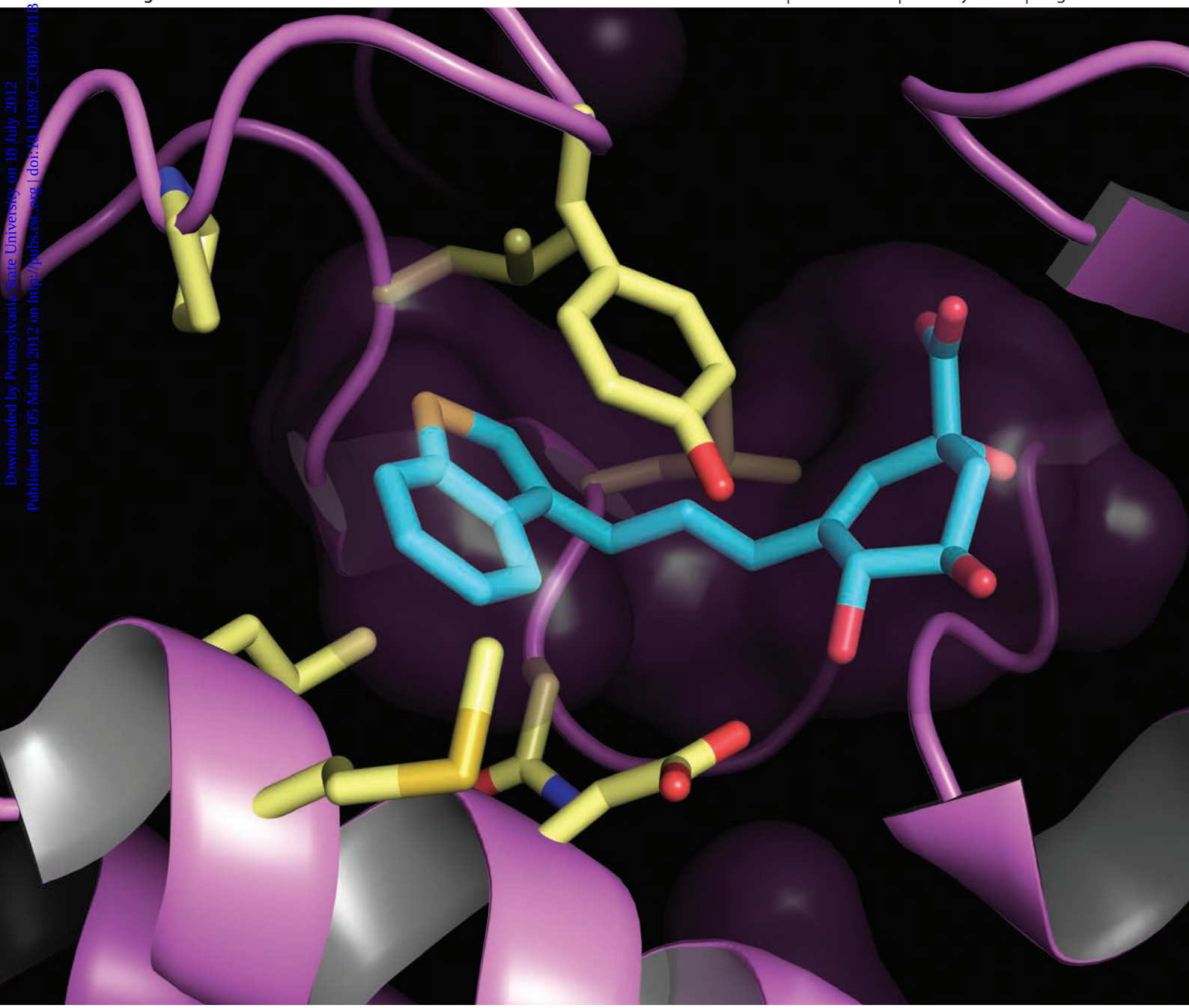

ISSN 1477-0520

RSC Publishing

PAPER

Concepción González-Bello *et al.*

Synthesis of 3-alkyl enol mimics inhibitors of type II dehydroquinase: factors influencing their inhibition potency

Organic & Biomolecular Chemistry

Cite this: *Org. Biomol. Chem.*, 2012, **10**, 3662

www.rsc.org/obc

PAPER

Synthesis of 3-alkyl enol mimics inhibitors of type II dehydroquinase: factors influencing their inhibition potency†‡

Beatriz Blanco,[a] Antía Sedes,[a] Antonio Peón,[a] Heather Lamb,[b] Alastair R. Hawkins,[b] Luis Castedo[c] and Concepción González-Bello*[a]

Received 12th December 2011, Accepted 1st March 2012
DOI: 10.1039/c2ob07081b

Several 3-alkylaryl mimics of the enol intermediate in the reaction catalyzed by type II dehydroquinase were synthesized to investigate the effect on the inhibition potency of replacing the oxygen atom in the side chain by a carbon atom. The length and the rigidity of the spacer was also studied. The inhibitory properties of the reported compounds against type II dehydroquinase from *Mycobacterium tuberculosis* and *Helicobacter pylori* are also reported. The binding modes of these analogs in the active site of both enzymes were studied by molecular docking using GOLD 5.0 and dynamic simulations studies.

Introduction

In recent years, we have been working on the development of new antibiotics for the treatment of bacterial infections,[1] by inhibition of type II dehydroquinase (DHQ2), which catalyzes the reversible dehydration of 3-dehydroquinic acid (**1**) to form 3-dehydroshikimic acid (**2**) (Scheme 1).[2,3] The reaction proceeds through an enol intermediate **3**, which is stabilized by a conserved water molecule that interacts through hydrogen bonding to Asn12, the carbonyl group of Pro11, and the main-chain amide of Gly78. The final step is the acid-catalyzed elimination of the C-1 hydroxyl group – a reaction mediated by a histidine residue, which acts as a proton donor.[4]

In particular, we have focused on the inhibition of two pathogenic bacteria, *Mycobacterium tuberculosis*, the causative agent of tuberculosis and *Helicobacter pylori*, the causative agent of gastric and duodenal ulcers, which has also been classified as a type I carcinogen. We recently showed that 3-methoxyaryl derivatives **4a–c** (Fig. 1), in which the aryl moiety is linked to the cyclohexene core by a methoxy group, are potent competitive inhibitors of DHQ2 from *Helicobacter pylori* (DHQ2-Hp) and *Mycobacterium tuberculosis* (DHQ2-Mt).[5]

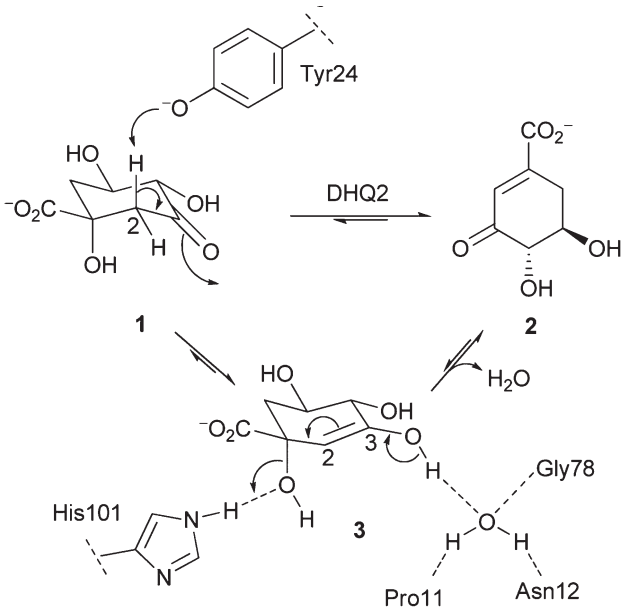

Scheme 1 Enzymatic conversion of 3-dehydroquinic acid (**1**) to 3-dehydroshikimic acid (**2**) catalyzed by DHQ2. The reaction proceeds *via* an enol intermediate **3**. Relevant residues are indicated (the numbering corresponds to *M. tuberculosis*).

The crystal structures of DHQ2-Hp and DHQ2-Mt in complex with compound **4c** have been solved at 2.95 Å and 1.5 Å, respectively (Fig. 2).[5,6] These crystal structures clarified the role of the aromatic rings on C3, which block the entrance of the essential arginine side chain into the active site and cause an important change in the conformation and flexibility of the loop

[a]*Centro Singular de Investigación en Química Biológica y Materiales Moleculares (CIQUS), Universidad de Santiago de Compostela, calle Jenaro de la Fuente s/n, 15782 Santiago de Compostela, Spain. E-mail: concepcion.gonzalez.bello@usc.es; Fax: +34 881 815704; Tel: +34 881 815726*
[b]*Institute of Cell and Molecular Biosciences, Medical School, University of Newcastle upon Tyne, Catherine Cookson Building, Framlington Place, Newcastle upon Tyne NE2 4HH, UK*
[c]*Departamento de Química Orgánica, Facultad de Química, Universidad de Santiago de Compostela, 15782 Santiago de Compostela, Spain*

†Electronic supplementary information (ESI) available: Plots for inhibition data and extra data plots for Molecular dynamics simulations. See DOI: 10.1039/c2ob07081b

‡This paper is dedicated to Prof. Miguel A. Miranda on the occasion of his 60th birthday.

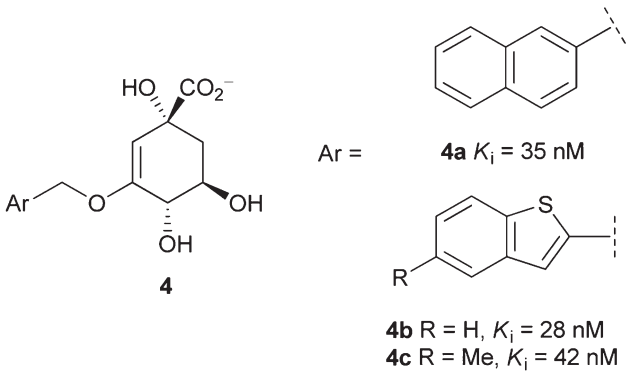

Fig. 1 Selected examples of 3-methoxyaryl derivatives that are DHQ2 competitive inhibitors. Inhibition constants against DHQ2-Mt are indicated.

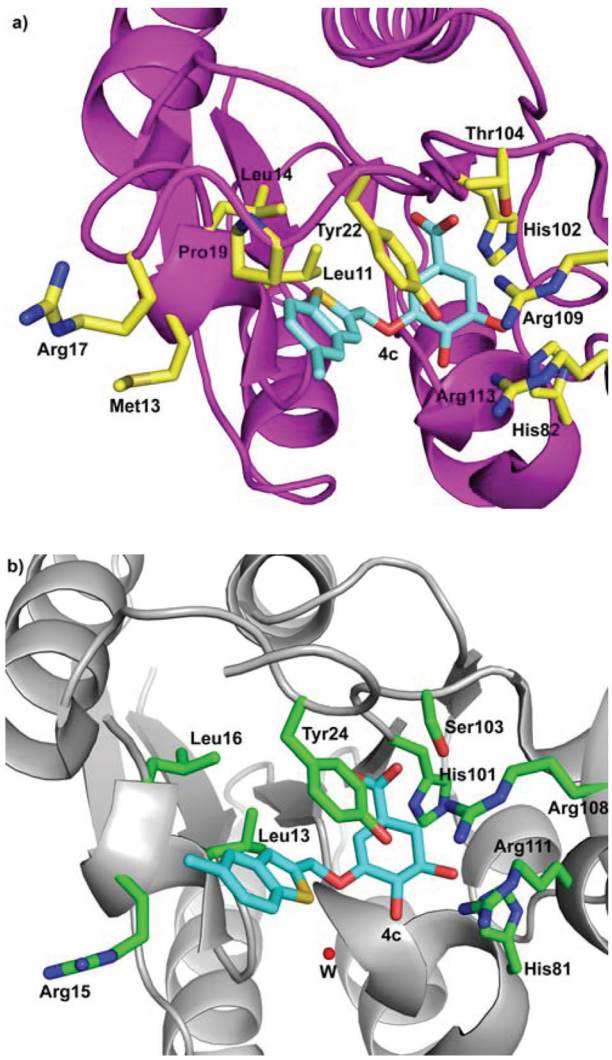

Fig. 2 Selected views of the crystal structures of the binary complex of: (a) DHQ2-Hp/**4c** (PDB: 2WKS, 2.95 Å);[5a] (b) DHQ2-Mt/**4c** (PDB: 2Y71, 1.5 Å).[5b] Relevant residues are indicated.

that closes over the substrate binding site. Molecular dynamics simulation studies suggest that the aromatic ring prevents appropriate orientation of the catalytic tyrosine of the loop for proton

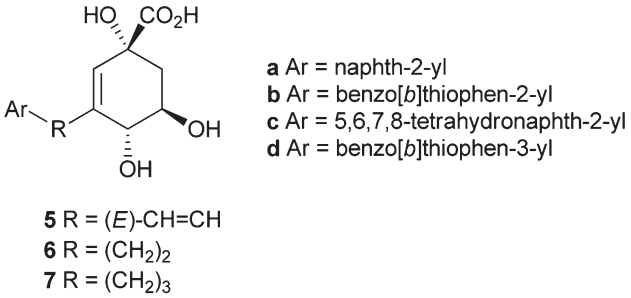

Fig. 3 Target compounds.

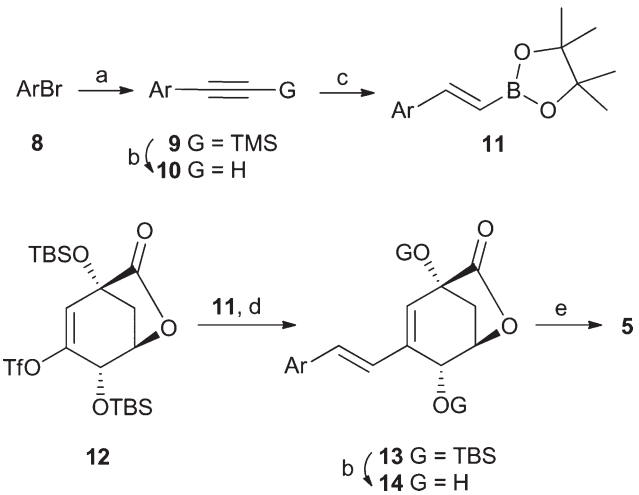

Scheme 2 The synthesis of compounds **5**. *Reagents and conditions*: (a) HCCTMS, CuI, $Pd(PPh_3)_2Cl_2$, Et_3N, 40 °C; (b) TBAF, THF, RT; (c) 1. Catechol borane, THF, Δ; 2. Pinacol, THF, Δ; (d) $Pd(PPh_3)_4$, K_3PO_4 (aq.), dioxane, 80 °C; (e) 1. LiOH, THF, RT; 2. Amberlite IR-120 (H^+).

abstraction and disrupts its basicity.[7] The crystal structure solved at 1.5 Å shows that the oxygen atom of the methylenoxy spacer of the inhibitor **4c** is located 3.1 Å away from the conserved water molecule involved in the catalysis (Fig. 2b). We assume that an important contribution of the high potency of the inhibitor, with K_i values of 42 nM[5b] and 130 nM[5a] against DHQ2-Mt and DHQ2-Hp, respectively, is due to the hydrogen-bonding interaction between the oxygen atom of the methylenoxy spacer with the conserved water molecule. In order to corroborate this hypothesis, we decided to investigate the effect on the inhibition potency of replacing the oxygen atom in the side chain of **4a–b** by a carbon atom. In addition, the length and the rigidity of the alkylene spacer was also studied. To this end, 3-alkylaryl enol mimics **5**, **6** and **7**, having a vinylene, ethylene and propylene spacer, respectively, were designed (Fig. 3). The results of inhibition studies of these compounds against DHQ2-Mt and DHQ2-Hp, docking studies using GOLD 5.0 and dynamic simulations studies are also described.

Results and discussion

Synthesis of vinylene derivatives 5

The synthesis of the target compounds **5** was achieved by Suzuki cross-coupling reactions between our previously reported

Table 1 The synthesis of compounds **9–11**, **13**, **14** and **5**[a]

Reaction	Comp	Yield (%)	Comp	Yield (%)
8 → 9	**9a**	99	**9b**	98
9 → 10	**10a**	98	**10b**	87
10 → 11	**11a**	85	**11b**	94
12 → 13	**13a**	94	**13b**	87
13 → 14	**14a**	65	**14b**	43
14 → 5	**5a**	77	**5b**	79

[a] **a** Ar = naphth-2-yl; **b** Ar = benzo[*b*]thiophen-2-yl.

Table 2 Synthesis of compounds **15–18** and **6**[a]

Reaction	Comp	Yield (%)	Comp	Yield (%)	Comp	Yield (%)
13 → 15	**15a**	75	**15b**	56	**15c**	20
13a → 15	**15a**	78	—	—	**15c**	0
12 → 15	**15a**	80	**15b**	80	—	—
15 → 16	**16a**	79	**16b**	60	**16c**	90
16 → 6	**6a**	85	**6b**	83	**6c**	85
8b → 17b	—	—	**17b**	96	—	—

[a] **a** Ar = naphth-2-yl; **b** Ar = benzo[*b*]thiophen-2-yl; **c** Ar = 5,6,7,8-tetrahydronaphth-2-yl.

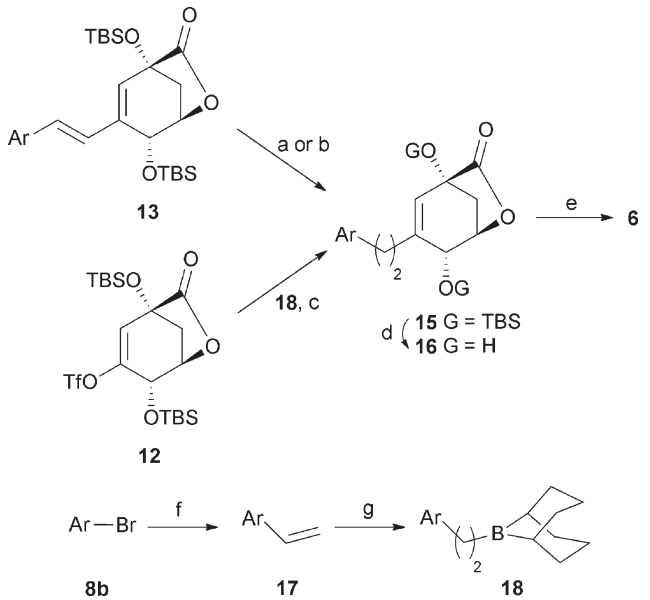

Scheme 3 Synthesis of acids **6**. *Reagents and conditions*: (a) H_2, Rosemund's catalyst, 50% THF–MeOH, RT; (b) H_2, RANEY-Ni®, 50% THF–MeOH, RT; (c) $PdCl_2(dppf)$, K_3PO_4, THF, Δ; (d) TBAF, THF, RT; (e) 1. LiOH, THF, RT; 2. Amberlite IR-120 (H^+); (f) vinyl boronic acid pinacol ester, $Pd(PPh_3)_4$, K_3PO_4 (aq.), dioxane, 80 °C; (g) 9-BBN-H, THF, 0 °C to RT.

vinyl triflate **12**[2c] and the appropriate boronic acid pinacol esters **11** (Scheme 2). Firstly, the Sonogashira cross-coupling reaction of commercially available aryl bromides **8** with trimethylsilylacetylene gave the protected alkynes **9**, which, by deprotection with TBAF, afforded terminal alkynes **10** (Scheme 2 and Table 1). Finally, hydroboration of alkynes **10** with catechol borane gave the required boronic acid pinacol esters **11** in good yield. Suzuki cross-coupling between vinyl triflate **12**[2c] and boronic acid pinacol esters **11** gave the corresponding cross-coupling products **13**, which were converted to the desired acids **5** by deprotection followed by basic hydrolysis of the corresponding lactones **14** and protonation with an ion-exchange resin.

Synthesis of ethylene derivatives 6

The synthesis of ethylene side-chain acids **6** was first addressed by selective reduction of the external double bond in dienes **13** (Scheme 3 and Table 2). Catalytic hydrogenation of **13** using Rosemund's catalyst gave the desired saturated derivatives **15a** and **15b** in 75% and 56% yield, respectively. Surprisingly, the reduction of naphthyl derivative **13a** also afforded a 20% yield of compound **15c** resulting from a partial reduction of the naphthyl moiety. However, this side reduction was avoided by using RANEY-Ni® as catalyst to afford compound **15a** as a single product in 78% yield. The tetrahydronaphthyl derivative **15c** was also transformed into its corresponding acid **6c** to test its biological activity.

The selective reduction of dienes **15** proved to be experimentally problematic due to the difficulty in controlling and monitoring the reduction. Because of that, we were particularly interested in addressing the synthesis of the alkyl lactones **15** by a direct sp^3–sp^2 cross-coupling reaction. After numerous attempts using various sp^3 boronic acids or their corresponding boronic acids pinacol esters, the cross-coupling was achieved by using alkyl boranes **18** and $PdCl_2(dppf)$ as catalyst in the presence of K_3PO_4 in THF.[8] Alkyl boranes **18** were synthesized by hydroboration with 9-BBN-H of vinyl derivatives **17**. Non-commercially available vinyl derivative **17b** was prepared by Suzuki cross-coupling of halide **8b** and vinyl boronic acid pinacol ester. Finally, compounds **15** were converted to the desired acids **6** in the same way as acids **5** from lactones **13**.

Synthesis of propylene derivatives 7

Our initial attempts to synthesize compounds **7** involved as the key step the Sonogashira cross-coupling between the triflate **12**[2c] and the terminal alkynes **20**, followed by selective reduction of the resulting enynes (Scheme 4 and Table 3). The required alkynes **20** were prepared by treatment of the Grignard derivative of **8** with (3-bromoprop-2-ynyl)trimethylsilane followed by deprotection. The latter reaction was achieved by treatment with $AgNO_3$ in ethanol as the usual TBAF or MeOH–K_2CO_3 conditions afforded allenes **21** in good yield.

A Sonogashira cross-coupling reaction between terminal alkynes **20** and triflate **12**[2c] in the presence of piperidine, a catalytic amount of copper iodide and $Pd(PPh_3)_4$ catalyst provided an excellent yield of the cross-coupling products **24**. The selective reduction of enynes **24** by catalytic hydrogenation using Rosemund's catalyst gave saturated side chain derivatives **25** in excellent yield. Alternatively, alkyl compounds **25** were synthesized by *B*-alkyl Suzuki cross-coupling between triflate **12**[2c] and alkyl boranes **23** using $Pd(PPh_3)_4$ as catalyst and in the presence of K_3PO_4. Alkyl boranes **23** were prepared by reaction of the Grignard derivative of **8** with allyl bromide followed by hydroboration with 9-BBN-H of the corresponding allyl

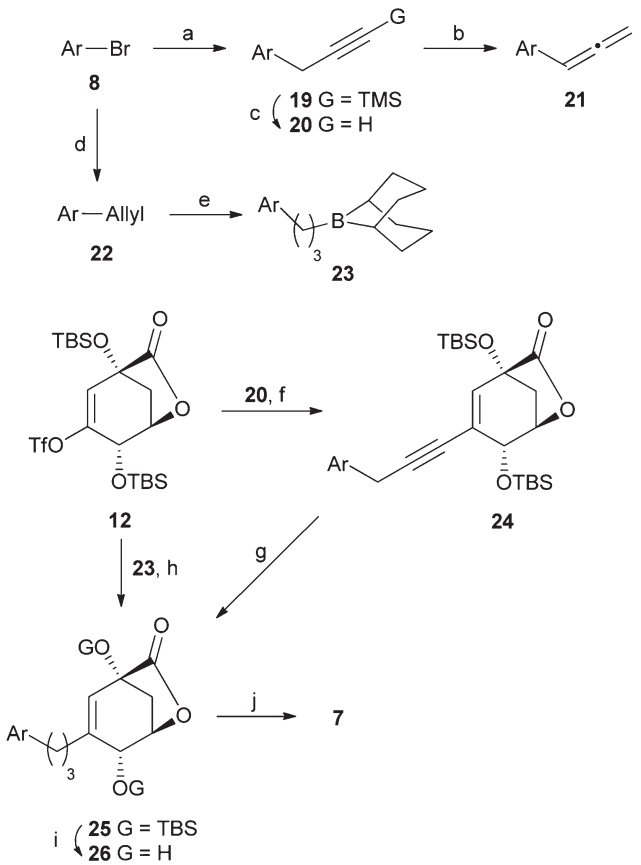

Scheme 4 Synthesis of compounds **7**. *Reagents and conditions*: (a) (1) Mg, I_2 (cat), THF, Δ. (2) TMSC≡CCH_2Br; (b) K_2CO_3, MeOH, 0 °C to RT; (c) $AgNO_3$, EtOH (aq.), RT; (d) (1) Mg, I_2 (cat), THF, Δ. (2) AllylBr; (e) 9-BBN-H, THF, 0 °C to RT; (f) $Pd(PPh_3)_4$, piperidine, CuI, THF, 40 °C; (g) H_2, Rosemund's catalyst, 50% THF–MeOH, RT; (h) $PdCl_2$(dppf), K_3PO_4, THF, Δ; (i) TBAF, THF, RT; (j) 1. LiOH, THF, RT; 2. Amberlite IR-120 (H^+).

Table 3 Synthesis of compounds **19–26** and **7**[a]

Reaction	Comp	Yield (%)	Comp	Yield (%)
8 → 19	**19a**	54	**19d**	69
19a → 21a	**21a**	91	—	—
19 → 20	**20a**	72	**20d**	61
8 → 22	**22a**	99	**22d**	89
12 → 24	**24a**	98	**24d**	95
24 → 25	**25a**	98	**25d**	98
12 → 25	**25a**	70	**25d**	42
25 → 26	**26a**	77	**26d**	67
26 → 7	**7a**	94	**7d**	87

[a] **a** Ar = naphth-2-yl; **d** Ar = benzo[*b*]thiophen-3-yl.

derivative **22**. Finally, compounds **25** were converted to the desired acids **7** in the same way as acids **5** from lactones **13**.

Inhibition assay results

The inhibitory properties of compounds **5–7** against DHQ2-Hp and DHQ2-Mt were tested. These compounds proved to be reversible competitive inhibitors of both enzymes. The inhibition data (K_i) are summarised in Table 4.

Table 4 K_i (nM) values for compounds **5–7** against DHQ2-Hp and DHQ2-Mt

Entry	Comp	R	*H. pylori*[a]	*M. tuberculosis*[b]
1	**5a**	(*E*)CH═CH	1400 ± 98	780 ± 94
2	**5b**	(*E*)CH═CH	3110 ± 249	520 ± 31
3	**6a**	$(CH_2)_2$	790 ± 29	436 ± 13
4	**6b**	$(CH_2)_2$	2460 ± 197	254 ± 20
5	**6c**	$(CH_2)_2$	1150 ± 115	274 ± 16
6	**7a**	$(CH_2)_3$	243 ± 19	180 ± 9
7	**7d**	$(CH_2)_3$	295 ± 10	73 ± 4
8	**4a**	OCH_2	310 ± 46[5b]	35 ± 2[5b]
9	**4b**	OCH_2	132 ± 13[5a]	28 ± 2[5b]

[a] Assay conditions: pH 7.0, 25 °C, 50 mM Tris·HCl. [b] Assay conditions: pH 7.0, 25 °C, 50 mM Tris·HOAc.

The biological results show that, in general, the effects of type, geometry and size of spacer were more pronounced in the inhibition potency against the DHQ2-Hp enzyme and in all cases the propylene spacer was the most potent of the series for both enzymes. In general, compounds **6** and **7**, having a flexible spacer, proved to be more potent than compounds **5** with a more rigid one (Table 4, entry 6 *vs*. 1). Benzothiophene **7d**, having a propylene spacer, was the most potent compound in the series, with K_i values of 73 nM and 295 nM against DHQ2-Mt and DHQ2-Hp, respectively. Naphthyl derivative **7a** also showed a high affinity against both enzymes, with K_i values of 180 nM and 243 nM against DHQ2-Mt and DHQ2-Hp, respectively. In addition, tetrahydronaphthalene **6c** proved to have binding affinities against DHQ2 in the same range as the other unsaturated analogs **6a–b** (Table 4, entry 5 *vs*. 3). In order to get an insight of the binding mode of these inhibitors, docking studies using GOLD 5.0.1[9] were carried out, which are discussed below.

Docking studies

The binding modes of inhibitors **5–7** with DHQ2 enzymes were studied using GOLD 5.0.1[9] with the enzyme geometries found in crystals of DHQ2-Hp and DHQ2-Mt binding to 3-methoxyaryl derivative **4c** (PDB code: 2WKS[5a] and 2Y71,[5b] respectively).

In general, 3-alkylaryl enol mimics with a three-carbon-atom spacer, as in ligands **7**, fit more efficiently into the active site than the corresponding ethylene ones (ligands **6**) because they locate the aromatic ring closer to the aliphatic residues of the enzyme active site (leucine pocket). This fact may account for the higher inhibition potency of propylene derivatives **7** relative to inhibitors **5** and **6**. The GOLD-predicted binding mode of one of the most active ligands of the 3-alkylaryl series, compound **7d**, in the active site of both enzymes is shown in Fig. 4. These docking studies show that this inhibitor should have similar polar interactions, through hydroxyl and carboxylate groups (not shown), to other mimetics of the enol intermediate, such as the ones present in the previously reported crystal structures (PDB code: 2WKS[5a] and 2Y71[5b]), because the cyclohexene ring occupies approximately the same position in the active site. More importantly, in both cases, the benzothiophene ring and the spacer are involved in a set of strong lipophilic interactions in this part of the active site. The benzothiophene moiety

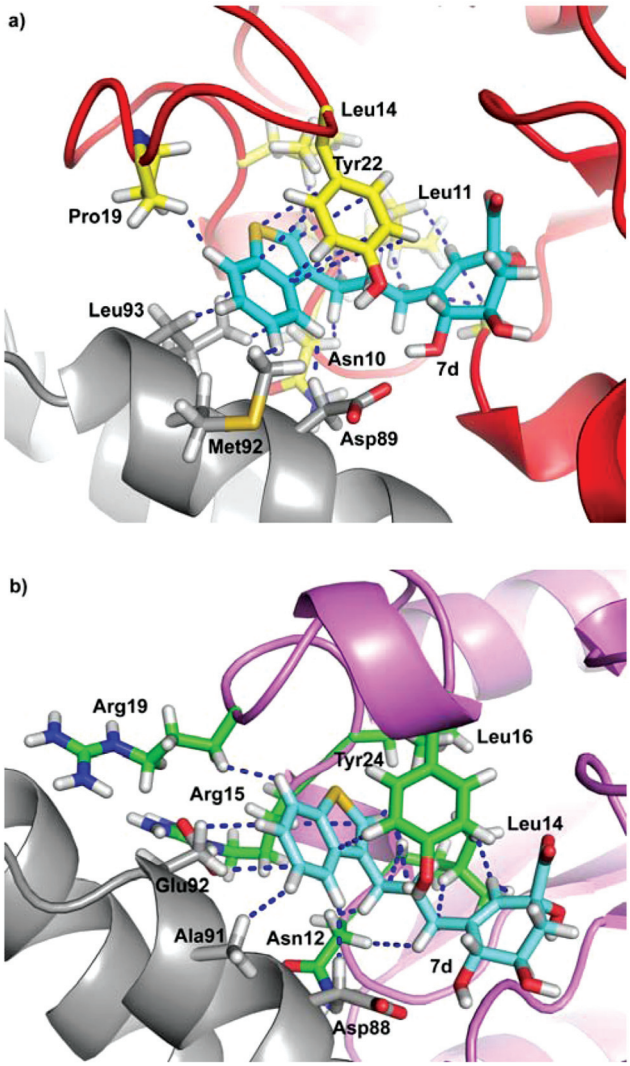

Fig. 4 GOLD-predicted binding for ligand **7d** to the active site of: (a) DHQ2-Hp (PDB: 2WKS[5a]); (b) DHQ2-Mt (PDB: 2Y71[5b]). Relevant residues are indicated. Symmetry-related neighboring chain close to the active site is indicated in gray.

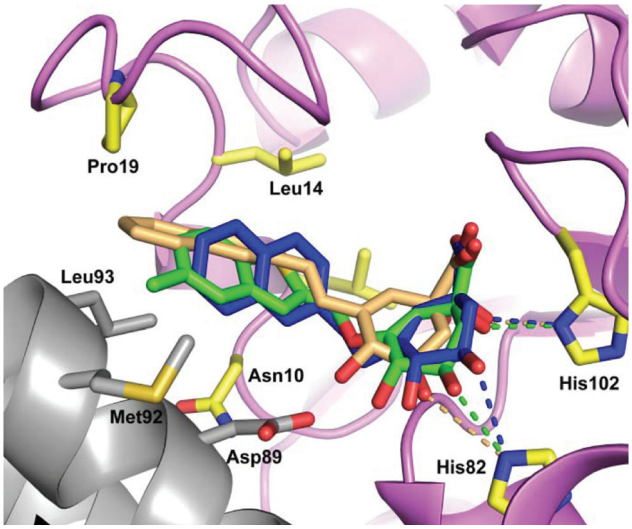

Fig. 5 Comparison of the position of inhibitor **4c** (green) in the enzyme–inhibitor crystal structure of DHQ2-Hp (PDB code: 2WKS[5a]) with the docking results of the highest score solution of ligands: **5a** (pale orange) and **6a** (blue). Relevant residues are indicated. The hydrogen bonding interactions of hydroxyl groups on C-1 and C-5 with His82 and His102 are highlighted as dotted lines with the same color as the corresponding ligand. Note how these contacts are much weaker for ligand **5a** than for compounds **6a** and **4c**.

interacts with the essential tyrosine by π stacking in DHQ2-Hp (Tyr22, Fig. 4a) and by an edge-face π–π interaction in DHQ2-Mt (Tyr24, Fig. 4b). This aromatic ring is also in close contact with the side chain of Leu14 and the five-membered ring of Pro19 in DHQ2-Hp and the side chain of Leu16, the carbon side chain of Arg15 and the essential Arg19 in DHQ2-Mt. The latter residues are located in the flexible loop that closes over the substrate binding site. The benzothiophene ring also interacts with some residues of a symmetry-related neighboring molecule (specifically, the side chains of Leu93, Met92 and Asp89 for DHQ2-Hp and the side chains of Ala91, Glu92 and Asp88 for DHQ2-Mt). The propylene moiety of **7d** interacts with the side chain of Leu11/Leu14, the carbon side chain of Asn10/Asn12 and carbon main chain of Gly78/Gly77 for DHQ2-Hp and DHQ2-Mt, respectively.

Comparison of saturated ligands **6** and the unsaturated ones **5** reveals that the saturated ones are predicted to be far more active than the corresponding unsaturated derivatives **5**, because the chain flexibility allows it to accommodate more adequately the aromatic ring in the active site, thus maximizing interactions (Fig. 5). In fact, the GOLD-predicted binding mode of ligand **5a** shows that the cyclohexene moiety is moved away from the polar contacts of the active site that anchors the six-membered ring of the substrate and the enol intermediate in the active site, *i.e.* His82, His101, *etc.* (Fig. 5). Even assuming that in a dynamic process the loop conformation and/or side chain residues might change, the ethylene spacer seems more suitable to maintain the polar interactions that anchor the cyclohexene moiety of the inhibitor.

Molecular dynamics simulations

On the other hand, the inhibition data clearly show that the replacement of the oxygen atom of the methylenoxy spacer by a carbon atom affords less potent inhibitors. This fact suggests that the oxygen atom of the spacer in compounds **4** is involved in a strong binding interaction with the essential water involved in the enzymatic mechanism, as described below. As shown in the recently solved crystal structure of the binary complex DHQ2-Mt/**4c**, the oxygen atom of the spacer is located 3.1 Å away from the essential water molecule (Fig. 2b). Therefore, this interaction should be lost on replacing the ether linkage by a methylene group. In order to corroborate this hypothesis and further analyze the binding mode of these inhibitors in the active site of the DHQ2, we studied the binding mode of *O*-alkylaryl derivative **4c** and the corresponding *C*-alkylaryl derivative **6e** (Ar = 5-methylbenzo[*b*]thiophen-3-yl) by molecular dynamics simulations (MD). The results show that the position in the active site of 3-methoxybenzothiophenyl derivatives **4c**, which has a methylenoxy spacer, does not change significantly during the

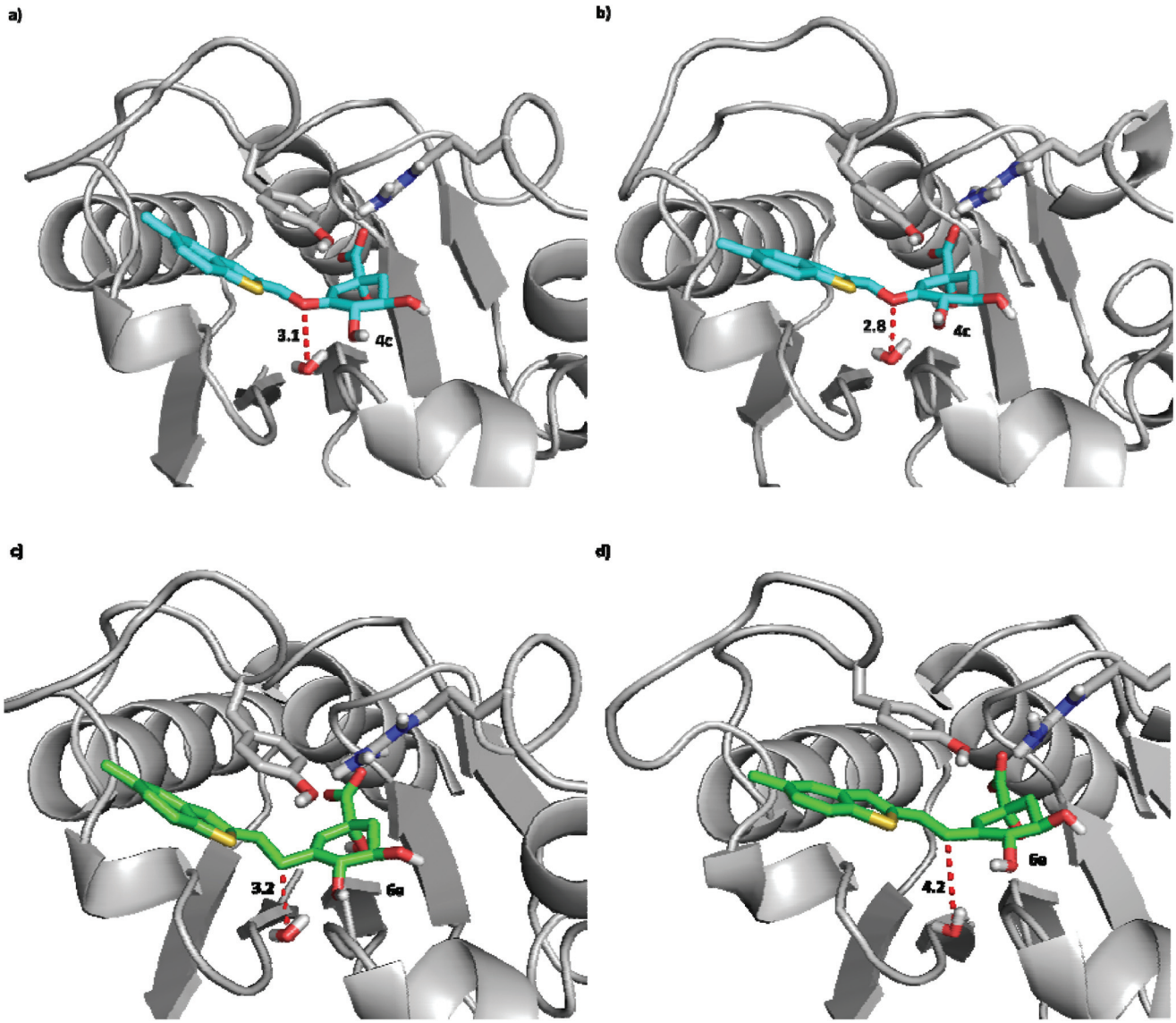

Fig. 6 Binding mode of ligand **4c** (cyan) and ligand **6e** (green) in the active site of DHQ2-Mt obtained by MD simulations: (a and c) after minimization and previously to simulation; (b and d) after 10 ns of MD. Distance between the oxygen atom of the spacer of ligand **4c** (O6), the corresponding carbon atom in ligand **6e** (C8) and essential water molecule is indicated. Only relevant residues are indicated.

simulation (10 ns) – including its position relative to the catalytic water (Fig. 6a–b).

For 3-ethylbenzothiophenyl ligand **6e**, which contains an ethylene spacer, relevant changes were not found in the position of the cyclohexene moiety and therefore its polar contacts through hydroxyl and carboxylate groups with residues of the active site [His80, Arg111, Ser102, Asn74, His100, Asp89 (neighboring unit)]. However, an important change in the position and conformation of the side chain and the aromatic ring was observed. Both moieties are shifted significantly after the simulation, which causes a change in the position of the loop because the volume occupied by the ligand **6e** is now greater. As shown in Fig. 6, while the distance between the oxygen atom of the methylenoxy spacer in ligand **4c** does not change significantly after 10 ns of simulation (from 3.1 Å to 2.8 Å), the corresponding distance for ligand **6e** increases from 3.2 Å to 4.2 Å (see also ESI†). Therefore, the substitution of the methylenoxy spacer by an alkylene one might cause the loss of a favorable polar interaction between the ligand and the catalytic water and this in turn causes a loss of inhibition potency.

Conclusions

Several 3-alkylaryl mimics of the enol intermediate in the reaction catalyzed by the third enzyme of the shikimic acid pathway, *i.e.* type II dehydroquinase – an essential enzyme in *M. tuberculosis* and *H. pylori*, were synthesized and tested as inhibitors of these enzymes. Vinylene derivatives **5** were synthesized by Suzuki cross-coupling reactions between previously reported triflate **12**[2c] and boronic acids pinacol esters **11** as the key step. 2- and 3-Alkylaryl enol mimics **6** and **7** were synthesized by *B*-alkyl Suzuki cross-coupling reactions using alkyl boranes **18** and **23**, respectively. Ethylene **6** and propylene side-chain acids **7** were also synthesized by selective catalytic

hydrogenation using Rosemund's catalyst or RANEY-Ni® of the external double and triple bond in dienes **13** and enynes **24**, respectively, which were obtained by Suzuki and Sonogashira cross-coupling reactions.

The reported compounds were synthesized to evaluate the contribution to the high potency of inhibitors **4** of the hydrogen-bonding interaction between the oxygen atom of the methylenoxy spacer and the essential water involved in the catalysis, as well as the length and the rigidity of the alkylene spacer. The biological results show that the replacement of the oxygen atom of the methylenoxy spacer of previously reported inhibitors **4a**[5a] and **4c**[5b] by a carbon atom leads to a decrease in the inhibition potency of up to 20-fold. The inhibition data together with the molecular dynamics simulation studies performed show that this hydrogen-bonding interaction has an important contribution on the inhibition potency of inhibitors **4** and it should therefore be considered in future designs. In general, effects of geometry and size of the alkyl spacer were more pronounced in the inhibition potency against the DHQ2-Hp enzyme and in all cases compounds **6** and **7** having a flexible spacer proved to be more potent than compounds **5** with a more rigid one. Docking studies using the program GOLD 5.0.1 suggest that compounds with a three-carbon spacer fit more efficiently into the active site because they locate the aromatic ring closer to the aliphatic residues of the enzyme active site.

Experimental

General

All starting materials and reagents were commercially available and were used without further purification. ^{1}H NMR spectra (250, 300, 400 and 500 MHz) and ^{13}C NMR spectra (63, 75, 100 and 125 MHz) were measured in deuterated solvents. *J* values are given in Hertz. NMR assignments were carried out by a combination of 1 D, COSY, and DEPT-135 experiments. FT-IR spectra were recorded as NaCl plates or KBr discs. $[\alpha]_{20}^{D}$ = values are given in 10^{-1} deg cm^2 g^{-1}. All procedures involving the use of ion-exchange resins were carried out at room temperature using Milli-Q deionized water. Amberlite IR-120 (H^+) (cation exchanger) was washed alternately with water, 10% NaOH, water, 10% HCl, and finally water before use. HPLC was performed on a semipreparative column (Phenomenex Luna, 250 × 21.2 mm, C18), eluting with acetonitrile–water at a flow rate of 7 mL min^{-1}.

Trimethyl(3-(naphthalen-2-yl)ethynyl)silane (9a)

A Schlenk tube was charged with 2-bromonaphthalene (**8a**) (500 mg, 2.41 mmol), $Pd(PPh_3)_2Cl_2$ (105 mg, 0.14 mmol), CuI (25 mg, 0.14 mmol) and dry triethylamine (5 mL). The resulting solution was deoxygenated and ethynyltrimethylsilane (0.5 mL, 3.62 mmol) was added dropwise. After addition of the first drop, the reaction color changed from yellow to black. The resulting solution was heated at 40 °C for 5 h. After cooling to room temperature, saturated ammonium chloride (0.5 mL) was added and the reaction mixture was extracted with diethyl ether (×3). The combined organic extracts were dried (anh. Na_2SO_4), filtered and concentrated under reduced pressure. The residue obtained was purified by flash chromatography on silica gel, eluting with hexanes to give silane **9a** (534 mg, 99%) as a brown oil. δ_H (250 MHz; $CDCl_3$): 8.19 (1 H, br s, ArH), 7.90–7.83 (3 H, m, 3 × ArH), 7.70 (1 H, dd, *J* = 7.5 and 1.5 Hz, ArH), 7.56 (2 H, dd, *J* = 6.3 and 3.2 Hz, 2 × ArH) and 0.52 (9 H, s, 3 × $SiCH_3$); δ_C (63 MHz; $CDCl_3$): 133.0 (2 × C), 132.1 (CH), 128.6 (CH), 128.0 (2 × CH), 127.8 (CH), 126.8 (CH), 126.6 (CH), 120.5 (C), 106.8 (C), 95.6 (C) and 0.2 (3 × $SiCH_3$); ν_{max} (film)/cm^{-1} 2152 (C≡C).

(Benzo[*b*]thiophen-2-ylethynyl)trimethylsilane (9b)

The experimental procedure used was the same as for alkyne **9a** utilizing 2-bromobenzo[*b*]thiophene (**8b**) (1 g, 4.69 mmol). Yield = 1.05 g (98%). White solid. Mp: 57–58 °C; δ_H (250 MHz; $CDCl_3$): 7.81–7.75 (2 H, m, 2 × ArH), 7.52 (1 H, br s, ArH), 7.41–7.37 (2 H, m, 2 × ArH) and 0.37 (9 H, s, 3 × $SiCH_3$); δ_C (63 MHz; $CDCl_3$): 140.2 (C), 139.0 (C), 129.6 (CH), 125.6 (CH), 124.8 (CH), 124.0 (CH), 123.2 (C), 122.1 (CH), 101.1 (C), 98.0 (C), and 0.1 (3 × $SiCH_3$); ν_{max} (KBr)/cm^{-1} 2143 (C≡C); MS (ESI) *m/z* 231 (MH^+); HRMS (ESI) calcd for $C_{13}H_{15}SSi$ (MH^+): 231.0658, found 231.0666.

2-Ethynylnaphthalene (10a)

Tetrabutylammonium fluoride (2.9 mL, 2.87 mmol, *ca.* 1.0 M in THF) was added to a stirred solution of the silyl ether **9a** (534 mg, 2.39 mmol) in dry THF (25 mL) under argon at room temperature. After stirring for 1 h the solvent was removed under reduced pressure and the residue was dissolved in ethyl acetate and HCl (10%). The organic layer was separated and the aqueous layer was extracted with ethyl acetate (×2). The combined organic extracts were dried (anh. Na_2SO_4), filtered and concentrated under reduced pressure. The residue was purified by flash chromatography on silica gel, eluting with hexanes to yield alkyne **10a** (354 mg, 98%) as a colorless oil. δ_H (250 MHz; $CDCl_3$): 8.19 (1 H, s, ArH), 7.92–7.85 (3 H, m, 3 × ArH), 7.71 (1 H, dd, *J* = 8.5 and 1.6 Hz, ArH), 7.60–7.57 (2 H, m, ArH) and 3.36 (1 H, s, CH); δ_H (63 MHz; $CDCl_3$): 133.0 (C), 132.8 (C), 132.3 (CH), 128.5 (CH), 128.0 (CH), 127.7 (2 × CH), 126.9 (CH), 126.6 (CH), 119.4 (C), 84.1 (C) and 77.7 (CH); ν_{max} (KBr)/cm^{-1} 2104 (C≡C).

2-Ethynylbenzo[*b*]thiophene (10b)

The experimental procedure used was the same as for 2-ethynylnaphthalene (**10a**) utilizing silyl ether **9b** (1.05 g, 4.58 mmol). Yield = 630 mg (87%). Red liquid. δ_H (250 MHz; $CDCl_3$): 7.84–7.78 (2 H, m, 2 × ArH), 7.58 (1 H, s, ArH), 7.45–7.41 (2 H, m, 2 × ArH) and 3.53 (1 H, s, CH); δ_C (63 MHz; $CDCl_3$): 140.1 (C), 138.7 (C), 130.1 (CH), 125.8 (CH), 124.8 (CH), 124.0 (CH), 122.0 (CH), 121.9 (C), 83.2 (C) and 77.3 (CH); ν_{max} (film)/cm^{-1} 2100 (C≡C).

(*E*)-4,4,5,5-Tetramethyl-2-(2-(naphth-2-yl)vinyl)-1,3,2-dioxaborolane (11a)

A Schlenk tube was charged with 2-ethynylnaphthalene (**10a**) (1.54 g, 10.14 mmol), catecholborane (1.28 mL, 11.15 mmol)

and dry THF (2 mL). The resultant solution was heated under reflux for 12 h. After cooling to room temperature, a solution of pinacol (3.85 g, 32.57 mmol) in dry THF (20 mL) was added. The reaction mixture was heated under reflux for 19 h. After cooling to room temperature, the solvent was removed under reduced pressure. The residue was purified by flash chromatography on silica gel, preneutralized with (1 : 2 : 97) triethylamine–diethyl ether–hexanes, using (3 : 97) diethyl ether–hexanes as eluent, to give boronic acid pinacol ester **11a** (2.43 g, 85%) as a yellow oil. δ_H (250 MHz; $CDCl_3$): 7.83 (4 H, m, 4 × ArH), 7.61 (1 H, d, J = 18.5 Hz, C*H*═CHB), 7.48 (3 H, m, 3 × ArH), 6.33 (1 H, d, J = 18.5 Hz, CH═C*H*B), 1.36 (9 H, s, 3 × CH_3) and 1.24 (3 H, s, CH_3); δ_C (63 MHz; $CDCl_3$): 149.5 (CH), 134.9 (C), 133.7 (C), 133.4 (C), 128.4 (CH), 128.2 (CH), 128.0 (CH), 127.6 (2 × CH), 126.4 (CH), 126.2 (CH), 124.9 (CH), 123.3 (CH), 83.3 (2 × C) and 24.8 (4 × CH_3).

(*E*)-2-(2-(Benzo[*b*]thiophen-2-yl)vinyl)-4,4,5,5-tetramethyl-1,3,2-dioxaborolane (11b)

The experimental procedure used was the same as for dioxaborolane **11a** utilizing alkyne **10b** (600 mg, 3.79 mmol). Yield: 1.03 g (94%). Yellow oil. δ_H (250 MHz; $CDCl_3$): 7.84–7.76 (2 H, m, 2 × ArH), 7.69 (1 H, d, J = 18.0 Hz, C*H*═CHB), 7.35–7.32 (2 H, m, 2 × ArH), 7.29 (1 H, s, ArH), 6.16 (1 H, d, J = 18.0 Hz, CH═C*H*B) and 1.38 (12 H, s, 4 × CH_3); δ_C (63 MHz; $CDCl_3$): 143.8 (C), 142.3 (CH), 139.8 (C), 139.5 (C), 125.2 (CH), 125.0 (CH), 124.4 (CH), 123.9 (2 × CH), 122.2 (CH), 83.3 (2 × C) and 24.7 (4 × CH_3).

(1*R*,4*R*,5*R*)-1,4-Di(*tert*-butyldimethylsilyloxy)-3-((*E*)-2-(naphth-2-yl)vinyl)cyclohex-2-en-1,5-carbolactone (13a)

A Schlenk tube was charged with triflate **12**[2c] (57 mg, 0.11 mmol), $Pd(PPh_3)_4$ (4.1 mg, 0.035 mmol) and dry dioxane (1 mL). K_3PO_4 (0.18 mL, 0.18 mmol, 1 M) and dioxaborolane **11a** (60 mg, 0.21 mmol) were added. The resultant solution was deoxygenated and heated at 80 °C for 3.5 h under argon. After cooling to room temperature, the solvent was removed under reduced pressure. The residue was dissolved in a mixture of dichloromethane and water. The organic layer was separated and the aqueous phase was extracted with dichloromethane (×2). The combined organic extracts were dried (Na_2SO_4), filtered and concentrated under reduced pressure. The residue obtained was purified by flash chromatography on silica gel, eluting with a gradient of dichloromethane–hexanes (15 : 85 to 25 : 75), to give naphthyl derivative **13a** (56 mg, 94%) as a white foam. $[\alpha]_{20}^{D}$ = −9.8° (c 1.0 in $CHCl_3$); δ_H (250 MHz; $CDCl_3$): 7.85–7.74 (4 H, m, 4 × ArH), 7.50–7.41 (3 H, m, 3 × ArH), 6.89 (1 H, d, J = 16.3 Hz, ArC*H*═CH), 6.70 (1 H, d, J = 16.3 Hz, ArCH═C*H*), 6.18 (1 H, s, H-2), 4.66 (1 H, m, H-5), 4.58 (1 H, d, J = 3.2 Hz, H-4), 2.55 (1 H, d, J = 10.6 Hz, H-6_{ax}), 2.41 (1 H, m, H-6_{eq}), 1.00 (9 H, s, $C(CH_3)_3$), 0.94 (9 H, s, $C(CH_3)_3$), 0.30 (3 H, s, $SiCH_3$), 0.28 (3 H, s, $SiCH_3$), 0.26 (3 H, s, $SiCH_3$) and 0.24 (3 H, s, $SiCH_3$); δ_C (63 MHz; $CDCl_3$): 175.4 (C), 136.7 (C), 134.1 (C), 134.1 (CH), 133.7 (C), 133.2 (C), 130.6 (CH), 128.5 (CH), 128.1 (CH), 127.8 (CH), 126.8 (2 × CH), 126.5 (CH), 126.2 (CH), 123.2 (CH), 83.2 (C), 75.3 (CH), 66.2 (CH), 37.2 (CH_2), 25.7 (2 × $C(CH_3)_3$), 18.1 (2 × $C(CH_3)_3$), −2.9 (2 × CH_3), −3.9 (CH_3) and −4.1 (CH_3); ν_{max} (film)/cm^{-1} 1799 (CO) cm^{-1}; MS (ESI) m/z = 559 (MNa^+); HRMS (ESI) calcd for $C_{31}H_{44}O_4SiNa$ (MNa^+): 559.2670, found 559.2670.

(1*R*,4*R*,5*R*)-3-((*E*)-2-(Benzo[*b*]thiophen-2-yl)vinyl)-1,4-di(*tert*-butyl-dimethylsilyloxy)cyclohex-2-en-1,5-carbolactone (13b)

The experimental procedure used was the same as for compound **13a** utilizing triflate **12**[2c] (355 mg, 0.67 mmol) and dioxaborolane **11b** (382 mg, 1.34 mmol). White foam. Yield = 315 mg (87%). $[\alpha]_{20}^{D}$ = −94.4° (c 1.0 in $CHCl_3$); δ_H (250 MHz; $CDCl_3$): 7.86–7.76 (2 H, m, 2 × ArH), 7.43–7.36 (2 H, m, 2 × ArH), 7.26 (1 H, s, ArH), 7.03 (1 H, d, J = 16.0 Hz, ArC*H*═CH), 6.54 (1 H, d, J = 16.0 Hz, ArCH═C*H*), 6.26 (1 H, s, H-2), 4.73 (1 H, dd, J = 3.3 and 5.2 Hz, H-5), 4.58 (1 H, d, J = 3.3 Hz, H-4), 2.60 (1 H, d, J = 10.6 Hz, H-6_{ax}), 2.55–2.42 (1 H, m, H-6_{eq}), 1.08 (9 H, s, $C(CH_3)_3$), 1.03 (9 H, s, $C(CH_3)_3$), 0.38 (3 H, s, CH_3), 0.36 (3 H, s, CH_3), 0.33 (3 H, s, CH_3) and 0.31 (3 H, s, CH_3); δ_C (63 MHz; $CDCl_3$): 175.2 (C), 142.2 (C), 140.1 (C), 139.1 (C), 136.0 (C), 134.5 (CH), 128.4 (CH), 125.0 (CH), 124.6 (C), 124.4 (CH), 123.8 (CH), 123.6 (CH), 122.3 (CH), 75.8 (CH), 75.2 (C), 66.3 (CH), 37.1 (CH_2), 25.7 (2 × $C(CH_3)_3$), 18.1 (2 × $C(CH_3)_3$), −2.9 (2 × CH_3), −3.9 (CH_3) and −4.3 (CH_3); ν_{max} (film)/cm^{-1} 1799 (CO); MS (ESI) m/z = 543 (MH^+); HRMS (ESI) calcd for $C_{29}H_{43}O_4SSi_2$ (MH^+): 543.2415, found 543.2404.

(1*R*,4*R*,5*R*)-1,4-Dihydroxy-3-((*E*)-2-(naphth-2-yl)vinyl)cyclohex-2-en-1,5-carbolactone (14a)

The experimental procedure used was the same as for alkyne **9a** utilizing silyl ether **13a** (290 mg, 0.54 mmol). Purification by flash chromatography over silica gel, eluting with (1 : 1) ethyl acetate–hexanes gave diol **14a** (107 mg, 65%) as a colorless oil. $[\alpha]_{20}^{D}$ = −95.7° (c 1.0 in MeOH); δ_H (250 MHz; CD_3OD): 7.80–7.75 (4 H, m, 4 × ArH), 7.64 (1 H, dd, J = 8.7 and 1.3 Hz, ArH), 7.44–7.39 (2 H, m, 2 × ArH), 7.11 (1 H, d, J = 16.4 Hz, ArC*H*═CH), 6.82 (1 H, d, J = 16.4 Hz, ArCH═C*H*), 6.16 (1 H, s, H-2), 4.73 (1 H, m, H-5), 4.54 (1 H, d, J = 3.2 Hz, H-4) and 2.49–2.41 (2 H, m, CH_2); δ_C (63 MHz; CD_3OD): 178.4 (C), 138.4 (C), 135.8 (C), 135.1 (C), 134.8 (CH), 134.6 (C), 132.2 (CH), 129.3 (CH), 129.0 (CH), 128.6 (CH), 128.3 (CH), 127.8 (CH), 127.4 (CH), 127.1 (CH), 124.3 (CH), 78.0 (CH), 74.5 (C), 65.8 (CH_2) and 37.6 (CH_2); ν_{max} (film)/cm^{-1} 3381 (OH) and 1772 (CO); MS (ESI) m/z = 331 (MNa^+); HRMS (ESI) calcd for $C_{19}H_{16}O_4Na$ (MNa^+): 331.0941, found 331.0934.

(1*R*,4*R*,5*R*)-3-((*E*)-2-(Benzo[*b*]thiophen-2-yl)vinyl)-1,4-dihydroxy-cyclohex-2-en-1,5-carbolactone (14b)

The experimental procedure used was the same as for diol **14a** utilizing silyl ether **13b** (315 mg, 0.58 mmol). Yield = 79 mg (43%). $[\alpha]_{20}^{D}$ = −82.4° (c 1.0 in MeOH); δ_H (250 MHz; CD_3OD): 7.78–7.67 (2 H, m, 2 × ArH), 7.31–7.17 (3 H, m, 3 × ArH), 7.22 (1 H, d, J = 16.0 Hz, ArC*H*═CH), 6.56 (1 H, d, J = 16.0 Hz, ArCH═C*H*), 6.14 (1 H, s, H-2), 4.71 (1 H, m, H-5), 4.49 (1 H, d, J = 3.3 Hz, H-4) and 2.44–2.35 (2 H, m, CH_2); δ_C

(63 MHz; CD_3OD): 178.2 (C), 143.7 (C), 141.6 (C), 140.4 (C), 138.0 (C), 135.6 (CH), 129.9 (CH), 126.1 (2 × CH), 125.7 (CH), 125.2 (CH), 124.6 (CH), 123.1 (CH), 78.0 (CH), 74.5 (C), 65.8 (CH) and 37.6 (CH_2); ν_{max} (film)/cm^{-1} 3427 (OH) and 1780 (CO); MS (ESI) m/z = 337 (MNa^+); HRMS (ESI) calcd for $C_{17}H_{14}O_4SNa$ (MNa^+): 337.0505, found 337.0494.

(1*R*,4*R*,5*R*)-1,4,5-Trihydroxy-3-((*E*)-2-(naphth-2-yl)vinyl) cyclohex-2-ene-1-carboxylic acid (5a)

A solution of the lactone **14a** (30 mg, 0.10 mmol) in THF (1 mL) and aqueous lithium hydroxide (0.5 mL, 0.25 mmol, 0.5 M) was stirred at room temperature for 10 min. Water was added and THF was removed under reduced pressure. The resulting aqueous solution was washed with diethyl ether (×2) and the aqueous extract was treated with Amberlite IR-120 until pH 6. The resin was filtered off and washed with Milli-Q water. The filtrate and the washings were lyophilised to give acid **5a** (25 mg, 77%) as a yellow solid. Mp: 197–199 °C; $[\alpha]_{20}^{D}$ = −48.2° (*c* 1.0 in MeOH); δ_H (250 MHz; CD_3OD): 7.75–7.61 (5 H, m, 5 × ArH), 7.37 (2 H, m, 2 × ArH), 7.02 (1 H, d, *J* = 16.3 Hz, ArC*H*═CH), 6.89 (1 H, d, *J* = 16.3 Hz, ArCH═C*H*), 5.80 (1 H, s, H-2), 4.36 (1 H, d, *J* = 3.3 Hz, H-4), 3.96 (1 H, m, H-5) and 2.17 (2 H, m, CH_2); δ_C (63 MHz; CD_3OD): 180.7 (C), 138.7 (C), 136.4 (C), 135.2 (C), 134.5 (C), 134.0 (CH), 130.9 (CH), 130.4 (CH), 129.2 (CH), 129.0 (CH), 128.6 (CH), 127.6 (CH), 127.3 (CH), 126.8 (CH), 124.5 (CH), 74.3 (C), 71.6 (CH), 68.8 (CH) and 35.9 (CH_2); ν_{max} (KBr)/cm^{-1} 3410 (OH) and 1651 (CO); MS (ESI) m/z = 325 ($M - H^+$); HRMS (ESI) calcd for $C_{19}H_{17}O_5$ ($M - H^+$): 325.1071, found 325.1078.

(1*R*,4*R*,5*R*)-3-((*E*)-2-(Benzo[*b*]thiophen-2-yl)vinyl)-1,4,5-trihydroxycyclohex-2-ene-1-carboxylic acid (5b)

The experimental procedure used was the same as for acid **5a** utilizing lactone **14b** (22.8 mg, 0.07 mmol). Yield = 18.4 mg (79%). Yellow solid. Mp: 184–185 °C; $[\alpha]_{20}^{D}$ = −41.6° (*c* 1.0 in MeOH); δ_H (250 MHz; CD_3OD): 7.67 (2 H, m, 2 × ArH), 7.22 (4 H, m, 3 × ArH + ArC*H*═CH), 6.63 (1 H, d, *J* = 16.0 Hz, ArCH═C*H*), 5.86 (1 H, s, H-2), 4.24 (1 H, d, *J* = 4.5 Hz, H-4), 3.99 (1 H, m, H-5) and 2.14 (2 H, m, CH_2); δ_C (63 MHz; CD_3OD): 178.8 (C), 144.6 (C), 141.7 (CH), 140.3 (C), 140.2 (C), 131.5 (C), 131.1 (CH), 125.9 (CH), 125.5 (CH), 124.7 (CH), 124.5 (CH), 123.0 (CH), 123.1 (CH), 71.4 (C), 71.1 (CH), 37.9 (CH_2) and 30.7 (CH); ν_{max} (KBr)/cm^{-1} 3435 (OH), 1639 (CO); MS (ESI) m/z = 331 ($M - H^+$); HRMS (ESI) calcd for $C_{17}H_{15}O_5S$ ($M - H^+$): 331.0635, found 331.0634.

Reduction of 13a with Rosemund's catalyst: preparation of (1*R*,4*R*,5*R*)-1,4-di(*tert*-butyldimethylsilyloxy)-3-(2-(naphthalen-2-yl)ethyl)cyclohex-2-en-1,5-carbolactone (15a) and (1*R*,4*R*,5*R*)-1,4-di(*tert*-butyldimethylsilyloxy)-3-(2-(5,6,7,8-tetrahydronaphthalen-2-yl)ethyl)cyclohex-2-en-1,5-carbolactone (15c)

A suspension of alkene **13a** (115 mg, 0.22 mmol) and Rosemund's catalyst (106 mg, 5% on weight) in a mixture of 50% THF–methanol (10 mL) was stirred under a hydrogen atmosphere at room temperature for 12 h. The mixture was filtered over Celite and the residue was washed with methanol. The filtrate and washings were evaporated. The obtained residue was purified by flash chromatography on silica gel, eluting with (1 : 2) dichloromethane–hexanes to yield naphthyl derivative **15a** (89 mg, 75%) and compound **15c** (23 mg, 20%). Data for **15a**: White foam. $[\alpha]_{20}^{D}$ = −6.5° (*c* 1.0 in $CHCl_3$); δ_H (250 MHz; $CDCl_3$): 7.86–7.80 (3 H, m, 3 × ArH), 7.62 (1 H, br s, ArH), 7.56–7.45 (2 H, m, 2 × ArH), 7.33 (1 H, dd, *J* = 8.4 and 1.6 Hz, ArH), 5.81 (1 H, s, H-2), 4.53 (1 H, m, H-5), 4.11 (1H, d, *J* = 3.1 Hz, H-4), 3.00–2.75 (3 H, m, CH_2 + C*H*H), 2.52–2.35 (3 H, m, CH_2 + CH*H*), 0.99 (9 H, s, $C(CH_3)_3$), 0.96 (9 H, s, $C(CH_3)_3$), 0.21 (3 H, s, CH_3), 0.18 (6 H, s, 2 × CH_3) and 0.15 (3 H, s, CH_3); δ_C (63 MHz; $CDCl_3$): 176.2 (C), 138.6 (C), 138.4 (C), 133.7 (C), 132.1 (C), 131.4 (CH), 128.1 (CH), 127.6 (CH), 127.6 (CH), 127.0 (CH), 126.5 (CH), 126.0 (CH), 125.3 (CH), 76.0 (CH), 74.8 (C), 68.0 (CH), 37.3 (CH_2), 33.9 (CH_2), 33.5 (CH_2), 25.7 (2 × $C(CH_3)_3$), 18.1 (2 × $C(CH_3)_3$), −3.0 (2 × CH_3) and −4.5 (2 × CH_3); ν_{max} (film)/cm^{-1} 1799 (C═O); MS (ESI) m/z = 561 (MNa^+); HRMS (ESI) calcd for $C_{31}H_{46}O_4Si_2Na$ (MNa^+): 561.2829, found 561.2823. Data for **15c**: Colorless oil. $[\alpha]_{20}^{D}$ = −3.2° (*c* 1.0 in $CHCl_3$); δ_H (250 MHz; $CDCl_3$): 7.09 (1 H, s, ArH), 6.99 (1 H, d, *J* = 7.9 Hz, ArH), 6.86 (1 H, m, ArH), 5.71 (1 H, s, H-2), 4.48 (1 H, m, H-5), 4.04 (1 H, d, *J* = 3.1 Hz, H-4), 2.74 (7 H, m, 3 × CH_2 + C*H*H), 2.33 (3 H, m, CH_2+C*H*H), 1.79 (4 H, m, 2 × CH_2), 0.93 (9 H, s, $C(CH_3)_3$), 0.92 (9 H, s, $C(CH_3)_3$), 0.17 (3 H, s, CH_3), 0.16 (3 H, s, CH_3), 0.15 (3 H, s, CH_3) and 0.13 (3 H, s, CH_3); δ_C (63 MHz; $CDCl_3$): 176.2 (C), 138.7 (C), 138.1 (C), 137.2 (C), 134.9 (C), 131.3 (CH), 129.3 (CH), 129.2 (CH), 125.5 (CH), 76.1 (CH), 74.8 (C), 67.9 (CH), 37.4 (CH_2), 33.8 (CH_2), 33.5 (CH_2), 29.5 (CH_2), 29.2 (CH_2), 25.8 ($C(CH_3)_3$), 25.8 ($C(CH_3)_3$), 25.7 (3 × CH_3), 23.4 (CH_2), 23.4 (CH_2), 18.0 (2 × $C(CH_3)_3$), −2.9 (2 × CH_3), −4.4 (CH_3) and −4.5 (CH_3); ν_{max} (film)/cm^{-1} 1799 (CO); MS (ESI) m/z = 565 (MNa^+); HRMS (ESI) calcd for $C_{31}H_{50}O_4Si_2Na$ (MNa^+): 561.3140, found 561.3128.

Reduction of 13a with RANEY-Ni®

A stirred solution of alkene **13a** (932 mg, 1.74 mmol) in 50% MeOH–THF (20 mL) was treated with an aqueous suspension of RANEY-Ni® (approx. 0.24 equivalents). The resulting suspension was deoxygenated and was stirred under hydrogen atmosphere at room temperature for 2.5 h. The mixture was filtered over Celite and the residue was washed with methanol. The filtrate and washings were evaporated. The obtained residue was purified by flash chromatography on silica gel, eluting with (5 : 95) acetone–hexanes to yield naphthyl derivative **15a** (731 mg, 78%).

(1*R*,4*R*,5*R*)-3-(2-(Benzo[*b*]thiophen-2-yl)ethyl)-1,4-di(*tert*-butyldimethylsilyloxy)cyclohex-2-en-1,5-carbolactone (15b)

The experimental procedure used was the same as for compound **15a** using Rosemund's catalyst and utilizing alkene **13b** (115.8 mg, 0.21 mmol). Yield = 65.2 mg (56%). Colorless oil. $[\alpha]_{20}^{D}$ = −88.3° (*c* 1.0 in $CHCl_3$); δ_H (250 MHz; $CDCl_3$): 7.77–7.65 (2 H, m, 2 × ArH), 7.34–7.22 (2 H, m, 2 × ArH),

6.98 (1 H, s, ArH), 5.78 (1 H, s, 1H, H-2), 4.48 (1 H, m, H-5), 4.07 (1 H, d, J = 3.1 Hz, H-4), 3.07–3.00 (2 H, m, CH_2), 2.47 (2 H, m, CH_2), 2.33 (2 H, m, CH_2), 0.93 (9 H, s, $C(CH_3)_3$), 0.90 (9 H, s, $C(CH_3)_3$), 0.18 (3 H, s, $SiCH_3$), 0.15 (3 H, s, $SiCH_3$), 0.12 (3 H, s, $SiCH_3$) and 0.09 (3 H, s, $SiCH_3$); δ_C (63 MHz; $CDCl_3$): 176.0 (C), 144.9 (C), 137.7 (C), 131.7 (CH), 128.5 (C), 124.3 (CH), 123.7 (CH), 123.0 (CH), 122.3 (CH + C), 121.1 (CH), 76.1 (CH), 74.9 (C), 68.2 (CH), 37.3 (CH_2), 33.5 (CH_2), 28.9 (CH_2), 25.8 (2 × C(CH_3)$_3$), 18.1 (2 × $C(CH_3)_3$), −2.9 (2 × CH_3), and −4.4 (2 × CH_3); ν_{max} (film)/cm^{-1} 1799 (CO); MS (ESI) m/z = 567 (MNa^+); HRMS (ESI) calcd for $C_{29}H_{44}O_4SSi_2Na$ (MNa^+): 567.2391, found 567.2390.

(1*R*,4*R*,5*R*)-1,4-Dihydroxy-3-(2-(naphth-2-yl)ethyl)cyclohex-2-en-1,5-carbolactone (16a)

The experimental procedure used was the same as for diol **14a** using silyl ether **15a** (89 mg, 0.16 mmol). Yield = 39 mg (79%). White foam. $[\alpha]_{20}^{D}$ = −89.6° (c 1.0 in MeOH); δ_H (250 MHz; CD_3OD): 7.76–7.69 (3 H, m, 3 × ArH), 7.53 (1 H, br s, ArH), 7.37 (2 H, m, 2 × ArH), 7.25 (1 H, dd, J = 8.4 and 1.6 Hz, ArH), 5.71 (1 H, s, H-2), 4.59 (1 H, m, H-5), 4.05 (1 H, d, J = 2.9 Hz, H-4), 2.92–2.79 (2 H, m, CH_2), 2.55–2.42 (2 H, m, CH_2) and 2.28 (2 H, m, CH_2); δ_C (63 MHz; CD_3OD): 179.0 (C), 140.6 (C), 140.1 (C), 135.1 (CH), 133.5 (C), 131.3 (CH), 128.9 (CH), 128.5 (2 × CH), 128.2 (CH), 127.5 (CH), 126.8 (CH), 126.2 (CH), 77.9 (CH), 73.9 (C), 67.6 (CH), 37.4 (CH_2) and 34.8 (2 × CH_2); ν_{max} (KBr)/cm^{-1} 3448 (OH) and 1776, 1761 and 1726 (CO); MS (ESI) m/z = 333 (MNa^+); HRMS (ESI) calcd for $C_{19}H_{18}O_4Na$ (MNa^+): 333.1097, found 333.1226.

(1*R*,4*R*,5*R*)-3-(2-(Benzo[*b*]thiophen-2-yl)ethyl)-1,4-dihydroxy-cyclohex-2-en-1,5-carbolactone (16b)

The experimental procedure used was the same as for diol **14a** utilizing silyl ether **15b** (65 mg, 0.12 mmol). Yield = 22 mg (60%). White foam. $[\alpha]_{20}^{D}$ = −78.4° (c 1.0 in MeOH); δ_H (250 MHz; CD_3OD): 7.72 (1 H, m, ArH), 7.64 (1 H, m, ArH), 7.11–7.28 (3 H, m, 3 × ArH), 5.76 (1 H, s, H-2), 4.60 (1 H, m, H-5), 4.01 (1 H, d, J = 3.1 Hz, H-4), 3.10–3.02 (1 H, m, C*H*H), 2.62–2.52 (3 H, m, CH_2 + CH*H*) and 2.26 (2 H, m, CH_2); δ_C (63 MHz; CD_3OD): 179.7 (C), 146.5 (C), 141.8 (C), 140.4 (C), 131.0 (CH), 129.8 (CH), 125.6 (CH), 125.0 (CH), 124.4 (CH), 123.4 (CH+C), 78.4 (CH), 74.4 (C), 68.0 (CH), 37.9 (CH_2), 35.0 (CH_2) and 29.9 (CH_2); ν_{max} (film)/cm^{-1} 3417 (OH), 1776 and 1770 (CO); MS (ESI) m/z = 339 (MNa^+); HRMS (ESI) calcd for $C_{17}H_{16}O_4SNa$ (MNa^+): 339.0662; found 339.0672.

(1*R*,4*R*,5*R*)-1,4-Dihydroxy-3-(2-(5,6,7,8-tetrahydronaphth-2-yl) ethyl)cyclohex-2-en-1,5-carbolactone (16c)

The experimental procedure used was the same as for diol **14a** utilizing ether **15c** (118 mg, 0.23 mmol). Yield: 65 mg (90%). White solid. Mp: 155.6–156.4 °C; $[\alpha]_{20}^{D}$ = −15.1° (c 1.0 in MeOH); δ_H (250 MHz; CD_3OD): 7.00 (1 H, s, ArH), 6.90–6.76 (2 H, m, 2 × ArH), 5.67 (1 H, s, H-2), 4.59 (1 H, m, H-4), 4.03 (1 H, m, H-5), 2.68 (7 H, m, 3 × CH_2 + C*H*H), 2.29 (3 H, m, 2 × CH_2 + C*H*H) and 1.76–1.73 (4 H, m, 2 × CH_2); δ_C (63 MHz; CD_3OD): 179.0 (C), 140.7 (C), 139.4 (C), 137.8 (C), 135.4 (C), 131.1 (CH), 130.0 (2 × CH), 126.6 (CH), 77.9 (CH), 73.9 (C), 67.4 (CH), 37.4 (CH_2), 35.1 (CH_2), 34.3 (CH_2), 30.2 (CH_2), 30.0 (CH_2), 24.5 (CH_2) and 24.4 (CH_2); ν_{max} (film)/cm^{-1} 3409 (OH) and 1764 (CO); MS (ESI) m/z = 337 (MNa^+); HRMS (ESI) calcd for $C_{19}H_{22}O_4Na$ (MNa^+): 337.1410, found 337.1414.

(1*R*,4*R*,5*R*)-1,4-Dihydroxy-3-(2-(naphth-2-yl)ethyl)cyclohex-2-ene-1-carboxylic acid (6a)

The experimental procedure used was the same as for acid **5a** utilizing lactone **16a** (24.3 mg, 0.08 mmol). Yield = 22 mg (85%). White solid. Mp: 120–122 °C; $[\alpha]_{20}^{D}$ = −8.3° (c 1.0 in MeOH); δ_H (250 MHz; CD_3OD): 7.79–7.73 (3 H, m, 3 × ArH), 7.65 (1 H, br s, ArH), 7.43–7.35 (3 H, m, 3 × ArH), 5.52 (1 H, s, H-2), 3.97–3.88 (2 H, m, H-4 + H-5), 3.06–3.98 (1 H, m, C*H*H), 2.91–2.82 (1 H, m, CH*H*), 2.75–2.68 (1 H, m, C*H*H), 2.49–2.41 (1 H, m, CH*H*) and 2.07 (2 H, m, CH_2); δ_C (63 MHz; CD_3OD): 178.3 (C), 145.0 (C), 140.8 (C), 135.1 (C), 133.5 (C), 128.8 (CH), 128.5 (2 × CH), 128.3 (CH), 127.4 (CH), 126.8 (CH), 126.1 (CH), 125.0 (CH), 74.9 (CH), 74.2 (C), 71.1 (CH), 40.3 (CH_2), 35.7 (CH_2) and 35.4 (CH_2); ν_{max} (film)/cm^{-1} 3435 (OH) and 1720 (CO); MS (ESI) m/z = 327 (M − H^+); HRMS (ESI) calcd for $C_{19}H_{19}O_5$ (M − H^+): 327.1227, found 327.1243.

(1*R*,4*R*,5*R*)-3-(2-(Benzo[*b*]thiophen-2-yl)ethyl)-1,4-dihydroxy-cyclohex-2-ene-1,5-carboxylic acid (6b)

The experimental procedure used was the same as for acid **5a** utilizing lactone **16b** (40 mg, 0.13 mmol). Yield = 36 mg (83%). White solid. Mp: 107–108 °C; $[\alpha]_{20}^{D}$ = −3.6° (c1.0 in MeOH); δ_H (250 MHz; CD_3OD): 7.72 (1 H, d, J = 7.0 Hz, ArH), 7.63 (1 H, d, J = 7.0 Hz, ArH), 7.25–7.12 (3 H, m, 3 × ArH), 5.43 (1 H, s, H-2), 3.87 (2 H, m, H-5 + H-4), 3.08 (1 H, m, C*H*H), 2.60 (1 H, m, CH*H*) and 2.09 (4 H, m, 2 × CH_2); δ_C (63 MHz; CD_3OD): 186.1 (C), 146.7 (C), 141.7 (C), 140.7 (C), 140.0 (CH), 131.7 (C), 125.0 (CH), 124.5 (CH), 123.8 (CH), 122.9 (CH), 122.0 (CH), 78.0 (CH), 74.0 (C), 68.0 (CH), 40.6 (CH_2), 35.3 (CH_2) and 30.0 (CH_2); ν_{max} (KBr)/cm^{-1} 3419 (OH) and 1778 (CO); MS (ESI) m/z = 333 (M − H^+); HRMS (ESI) calcd for $C_{17}H_{17}O_5S$ (M − H^+): 333.0791, found 333.0804.

(1*R*,4*R*,5*R*)-1,4,5-Trihydroxy-3-(2-(5,6,7,8-tetrahydronaphth-2-yl)ethyl)cyclohex-2-ene-1-carboxylic acid (6c)

The experimental procedure used was the same as for acid **5a** utilizing lactone **16c** (34.5 mg, 0.11 mmol). Yield = 31.2 mg (85%). Mp: 127–128 °C; $[\alpha]_{20}^{D}$ = −1.2° (c 1.0 in MeOH); δ_H (400 MHz; CD_3OD): 6.90 (2 H, m, 2 × ArH), 6.87 (1 H, m, ArH), 5.45 (1 H, s, H-2), 3.89 (2 H, m, H-5 + H-4), 2.78–2.74 (1 H, m, C*H*H), 2.71 (4 H, m, 2 × CH_2), 2.63–2.57 (2 H, m, CH_2), 2.29 (1H, m, CH*H*), 2.05 (2 H, m, CH_2), and 1.77 (4 H, m, 2 × CH_2); δ_C (63 MHz; CD_3OD): 178.4 (C), 145.2 (C), 140.2 (C), 137.8 (C), 135.3 (C), 122.9 (2 × CH), 126.6 (CH), 124.7 (CH), 74.8 (CH), 74.3 (C), 71.0 (CH), 40.3 (CH_2), 36.0 (CH_2), 34.9 (CH_2), 30.4 (CH_2), 30.0 (CH_2), 24.6 (CH_2), and 24.5 (CH_2); ν_{max} (KBr)/cm^{-1} 3427 (OH), 1701 (CO); MS (ESI) m/z = 331 (M − H^+); HRMS (ESI) calcd for $C_{19}H_{23}O_5$ (M − H^+): 331.1540, found 331.1543.

2-Vinylbenzo[*b*]thiophene (17b)

A Schlenk tube was charged with 2-bromobenzothiophene (**8b**)[10] (250 mg, 1.17 mmol), vinylboronic acid pinacol ester (0.3 mL, 1.73 mmol), $Pd(PPh_3)_4$ (67 mg, 0.06 mmol), aqueous K_2CO_3 (3.45 mL, 1.1 M) and dioxane (10 mL). The resulting solution was heated at 100 °C for 5 h. After cooling to room temperature, the reaction mixture was diluted with diethyl ether and water. The organic layer was separated and the aqueous phase was extracted with diethyl ether (×3). The combined organic extracts were dried (anh. Na_2SO_4), filtered and concentrated under reduced pressure. The residue was purified by flash chromatography on silica gel, eluting with (3 : 97) diethyl ether–hexanes to give 2-vinylbenzo[*b*]thiophene (**17b**)[11] (180 mg, 96%).

Preparation of 15a by *B*-alkyl Suzuki cross-coupling

(a) Preparation of borane 18a. A solution of 9-BBN-H (5.7 mL, 2.85 mmol, *ca.* 0.5 M in THF) was added to a flamed round-bottom flask under argon. After cooling to 0 °C, 2-vinylnaphthalene (**17a**) (200 mg, 1.29 mmol) was added. The mixture was warmed up slowly to room temperature and stirred for 3 h to give a solution of borane **18a**.

(b) *B*-alkyl Suzuki cross-coupling. To the borane solution obtained above, a solution of triflate **12**[2c] (200 mg, 0.37 mmol) in THF (4 mL), $PdCl_2$(dppf) (12.3 mg, 0.02 mmol) and aqueous K_3PO_4 (0.83 mL, 0.83 mmol, 1 M) were added. The resultant solution was heated at 70 °C for 4 h under argon. After cooling to room temperature, the solution was diluted with diethyl ether and water. The organic layer was separated and the aqueous phase was extracted with diethyl ether (×2). The combined organic extracts were dried (Na_2SO_4), filtered and concentrated under reduced pressure. The residue was purified by flash chromatography on silica gel, eluting with (5 : 95) diethyl ether–hexanes, to give compound **15a** (156 mg, 80%).

Trimethyl(3-(naphth-2-yl)prop-1-ynyl)silane (19a)

A two necked round bottom flask equipped with a condenser and a pressure compensated addition funnel was charged with magnesium turnings (141 mg, 5.82 mmol) and a few iodine pellets. The system was flamed under vacuum and cooled under an argon atmosphere. Dry THF (3 mL) was added to the round bottom flask and the compensated addition funnel was charged with a solution of 2-bromonaphthalene (**8a**) (1 g, 4.85 mmol) in dry THF (5 mL). This solution was slowly added to the suspension, which was heated under reflux for 2 h. The reaction mixture was cooled to room temperature and then it was treated with a solution of 3-bromoprop-1-ynyl)trimethylsilane (0.9 mL, 7.2 mmol) in dry THF (3 mL). The reaction mixture was heated under reflux for 2 h and then cooled to room temperature. Saturated NH_4Cl was added and the organic layer was separated. The aqueous phase was extracted with dichloromethane (×2). The combined organic extracts were dried (anh. Na_2SO_4), filtered and concentrated under reduced pressure. Purification by flash chromatography on silica gel, using hexanes as eluent, gave alkyne **19a** (621 mg, 54%) as a white solid. Mp: 61–63 °C; δ_H (400 MHz; $CDCl_3$): 7.85–7.80 (4 H, m, 4 × ArH), 7.50–7.44 (3 H, m, 3 × ArH), 3.82 (2 H, s, CH_2) and 0.24 (9 H, s, 3 × CH_3); δ_C (100 MHz; $CDCl_3$): 133.8 (C), 133.5 (C), 132.3 (C), 128.1 (CH), 127.6 (2 × CH), 126.4 (CH), 126.2 (CH), 126.1 (CH), 125.5 (CH), 104.2 (C), 87.2 (C), 26.4 (CH_2) and 0.11 (3 × CH_3); ν_{max} (KBr)/cm^{-1} 2173 (C≡C).

(3-(Benzo[*b*]thiophen-3-yl)prop-1-ynyl)trimethylsilane (19d)

The experimental procedure used was the same as for alkyne **19a** utilizing 3-bromobenzo[*b*]thiophene (**8d**) (1 g, 4.7 mmol) and (3-bromoprop-1-ynyl)trimethylsilane (0.9 mL, 5.6 mmol). Yield = 791 mg (69%). White solid. δ_H (250 MHz; $CDCl_3$): 7.90–7.86 (1 H, m, ArH), 7.76–7.74 (1 H, m, ArH), 7.45–7.37 (3 H, m, ArH), 3.81 (2 H, d, J = 1.25 Hz, CH_2) and 0.26 (9 H, s, 3 × CH_3); δ_C (63 MHz; $CDCl_3$): 140.6 (C), 137.9 (C), 130.6 (C), 124.3 (CH), 123.9 (CH), 123.0 (CH), 122.9 (CH), 121.3 (CH), 102.9 (C), 87.3 (C), 20.2 (CH_2) and 0.1 (3 × CH_3); ν_{max} (KBr)/cm^{-1} 2179 (C≡C); MS (CI) m/z = 245 (MH^+).

2-(Propa-1,2-dienyl)naphthalene (21a)

A stirred solution of silyl ether **19a** (30 mg, 0.13 mmol) in methanol (1.5 mL) at 0 °C was treated with potassium carbonate (17 mg, 0.13 mmol). The ice bath was removed and the resulting mixture was stirred for 1 h. The reaction mixture was partitioned in water and diethyl ether. The organic layer was separated and the aqueous phase was extracted with diethyl ether (×2). The combined organic extracts were dried (anh. Na_2SO_4), filtered and concentrated under reduced pressure. The residue was purified by flash chromatography on silica gel, eluting with (10 : 90) diethyl ether–hexanes to give allene **21a** (20 mg, 91%) as a white solid. Mp: 55.7–56.3 °C; δ_H (250 MHz; $CDCl_3$): 7.43–7.36 (3 H, m, 3 × ArH), 7.26 (1 H, s, ArH), 7.13–7.02 (3 H, m, 3 × ArH), 5.96 (1 H, t, J = 6.25 Hz, CH) and 4.83 (2 H, d, J = 5.0 Hz, CH_2); δ_C (75 MHz; $CDCl_3$): 210.5 (C), 133.8 (C), 132.7 (C), 131.5 (C), 128.4 (CH), 127.9 (CH), 127.8 (CH), 126.4 (CH), 125.8 (CH), 125.5 (CH), 124.8 (CH), 94.5 (CH) and 79.2 (CH_2); MS (CI) m/z = 167 [MH^+]; HRMS (CI) calcd for $C_{13}H_{11}$ (MH^+): 167.0861, found 167.0860.

2-(Prop-2-ynyl)naphthalene (20a)

A stirred solution of silyl silane **19a** (600 mg, 2.5 mmol) in ethanol (11 mL) was treated with a solution of $AgNO_3$ in (2.3 : 1) EtOH–H_2O (11 mL, 0.35 M). The resultant solution was stirred in the dark at room temperature for 2 h during which time a white solid was formed. An aqueous solution of potassium cyanide (3.3 mL, 7.6 M) was then added and the reaction mixture was stirred until disappearance of the white precipitate. Diethyl ether was added and the aqueous layer was separated. The organic extract was washed with brine, dried (anh. Na_2SO_4), filtered and concentrated under reduced pressure. The residue was purified by flash chromatography on silica gel, using hexanes as eluent, to give alkyne **20a** (297 mg, 72%) as a white solid. Mp: 52–53 °C; δ_H (250 MHz; $CDCl_3$): 7.84–7.81 (4 H, m, 4 × ArH), 7.51–7.44 (3 H, m, 3 × ArH), 3.79 (2 H, d, J = 1.5 Hz, CH_2) and 2.27 (1 H, t, J = 1.8 Hz, C≡CH); δ_C (63 MHz;

$CDCl_3$): 133.4 (2 × C), 132.3 (C), 128.2 (CH), 127.6 (2 × CH), 126.3 (CH), 126.2 (CH), 126.1 (CH), 125.6 (CH), 81.9 (C), 70.7 (CH) and 24.9 (CH_2); ν_{max} (KBr)/cm^{-1} 3282 (C≡C) cm^{-1}. MS (CI) m/z = 167 (MH^+); HRMS (CI) calcd for $C_{13}H_{11}$ (MH^+): 167.0861, found 167.0858.

3-(Prop-2-ynyl)benzo[*b*]thiophene (20d)

The experimental procedure used was the same as for alkyne **20a** utilizing silyl ether **19d** (1.6 g, 6.5 mmol). Yield = 657 mg (61%). Yellow oil. δ_H (250 MHz; $CDCl_3$): 8.00 (1 H, m, ArH), 7.91 (1 H, m, ArH), 7.79 (2 H, m, 2 × ArH), 7.58 (1 H, s, ArH), 3.79 (2 H, dd, J = 2.8 and 1.3 Hz, CH_2) and 2.29 (1 H, t, J = 2.8 Hz, C≡CH); δ_C (63 MHz; $CDCl_3$): 140.1 (C), 138.5 (C), 131.3 (C), 124.6 (CH), 124.3 (CH), 123.2 (CH), 122.8 (CH), 121.2 (CH), 80.6 (CH), 70.6 (C) and 18.8 (CH_2); ν_{max} (film)/cm^{-1} 3293 (C≡C); MS (CI) m/z = 173 (MH^+); HRMS (CI) calcd for $C_{11}H_9S$ (MH^+): 173.0425, found 173.0430.

2-Allylnaphthalene (22a)

The experimental procedure used was the same as for alkyne **19a** utilizing 2-bromonaphthalene (**8a**) (200 mg, 0.96 mmol) and allyl bromide (0.09 mL, 1 mmol). Yield = 158 mg (99%). Colorless oil. δ_H (300 MHz; $CDCl_3$): 7.91–7.85 (3 H, m, 3 × ArH), 7.71 (1 H, s, ArH), 7.58–7.40 (3 H, m, 3 × ArH), 6.23–6.07 (1 H, m, C*H*═CH_2), 5.28–5.19 (2 H, m, CH═CH_2) and 3.63 (2 H, d, J = 7.8 Hz, CH_2); δ_C (75 MHz; $CDCl_3$): 137.5 (C), 137.3 (CH), 133.6 (C), 132.1 (C), 127.9 (CH), 127.6 (CH), 127.4 (CH), 127.3 (CH), 126.6 (CH), 125.9 (CH), 125.2 (CH), 116.0 (CH_2) and 40.3 (CH_2); MS (CI) m/z = 169 (MH^+); HRMS (CI) calcd for $C_{13}H_{13}$ (MH^+): 169.1017, found 169.1023.

3-Allylbenzo[*b*]thiophene (22d)

The experimental procedure used was the same as for 2-allylnaphthalene (**22a**) utilizing 3-bromobenzo[*b*]thiophene (**8d**) (300 mg, 1.4 mmol). Yield = 218 mg (89%). Colorless oil. δ_H (250 MHz; $CDCl_3$): 8.05–7.86 (2 H, m, 2 × ArH), 7.58–7.38 (3 H, m, 3 × ArH), 6.28–6.15 (1 H, m, C*H*═CH_2), 5.36–5.27 (2 H, m, CH═CH_2) and 3.75 (2 H, m, CH_2); δ_C (63 MHz; $CDCl_3$): 140.5 (C), 138.8 (C), 135.5 (CH), 134.5 (C), 124.2 (CH), 123.8 (CH), 122.8 (CH), 122.1 (CH), 121.8 (CH), 116.6 (CH_2) and 33.0 (CH_2); MS (CI) m/z = 175 (MH^+); HRMS (CI) calcd for $C_{11}H_{11}S$ (MH^+): 175.0581, found 175.0582.

(1*R*,4*R*,5*R*)-1,4-Di(*tert*-butyldimethylsilyloxy)-3-(3-(naphth-2-yl)prop-1-ynyl)cyclohex-2-en-1,5-carbolactone (24a)

A Schlenk tube was charged with triflate **12**^{2c} (100 mg, 0.19 mmol) and dry THF (9.5 mL). CuI (7.6 mg, 0.04 mmol), $Pd(PPh_3)_4$ (45 mg, 0.04 mmol), 2-(prop-2-ynyl)naphthalene (**20a**) (158 mg, 0.95 mmol) and piperidine (0.25 mL, 2.47 mmol) were added. The resultant solution was deoxygenated and heated at 40 °C for 4 h. After cooling to room temperature, the reaction mixture was diluted with diethyl ether and water. The organic layer was separated and the aqueous phase was extracted with diethyl ether (×2). The combined organic extracts were washed with saturated solution of sodium bicarbonate (×2), dried (anh. Na_2SO_4), filtered and concentrated under reduced pressure. The residue was purified by flash chromatography on silica gel, eluting with a gradient of dichloromethane–hexanes (5 : 95 to 35 : 65), to give naphthyl derivative **24a** (102 mg, 98%) as an orange foam. $[\alpha]_{20}^{D}$ = −136° (*c* 1.0 in $CHCl_3$); δ_H (250 MHz; $CDCl_3$): 7.84–7.77 (4 H, m, 4 × ArH), 7.49–7.40 (3 H, m, 3 × ArH), 6.27 (1 H, s, H-2), 4.49 (1 H, m, H-5), 4.17 (1 H, d, J = 3.3 Hz, H-4), 3.88 (2 H, s, CH_2Ar), 2.38 (2 H, m, CH_2-6), 0.92 (9 H, s, $C(CH_3)_3$), 0.89 (9 H, s, $C(CH_3)_3$), 0.20 (3 H, s, $SiCH_3$), 0.16 (3 H, s, $SiCH_3$) and 0.12 (6 H, s, 2 × $SiCH_3$); δ_C (63 MHz; $CDCl_3$): 175.0 (C), 140.7 (CH), 133.5 (C), 133.4 (C), 132.3 (C), 128.3 (CH), 127.6 (CH), 127.6 (CH), 126.4 (CH), 126.3 (CH), 126.2 (CH), 125.6 (CH), 127.8 (C), 89.5 (C), 80.4 (C), 75.8 (CH), 74.9 (C), 68.2 (CH), 36.8 (CH_2), 25.8 (CH_2), 25.6 (2 × C(*C*H_3)$_3$), 18.0 (2 × *C*(CH_3)$_3$), −3.1 (2 × $SiCH_3$), −4.6 ($SiCH_3$) and −4.9 ($SiCH_3$); ν_{max} (KBr)/cm^{-1} 2225 (C≡C) and 1803 (CO) cm^{-1}; MS (ESI) m/z = 571 (MNa^+); HRMS (ESI) calcd for $C_{32}H_{44}Si_2O_4Na$ (MNa^+): 571.2670, found 571.2664.

(1*R*,4*R*,5*R*)-3-(3-(Benzo[*b*]thiophen-3-yl)prop-1-ynyl)-1,4-di(*tert*-butyldimethylsilyloxy)cyclohex-2-en-1,5-carbolactone (24d)

The experimental procedure used was the same as for naphthyl derivative **24a** using alkyne **20d** (164 mg, 0.95 mmol) and triflate **12**^{2c} (100 mg, 0.19 mmol). Yield = 100 mg (95%). Orange foam. $[\alpha]_{20}^{D}$ = −132° (*c* 1.0 in $CHCl_3$); δ_H (400 MHz; $CDCl_3$): 7.87 (1 H, m, ArH), 7.75 (1 H, m, ArH), 7.43–7.37 (2 H, m, 2 × ArH), 7.35 (1 H, s, ArH), 6.26 (1 H, d, J = 1.6 Hz, H-2), 4.48 (1 H, dd, J = 5.6 and 3.2 Hz, H-5), 4.14 (1 H, d, J = 3.2 Hz, H-4), 3.87 (2 H, s, CH_2Ar), 2.40 (1 H, d, J = 10.8 Hz, H-6_{ax}), 2.36 (1 H, ddd, J = 10.8, 5.6 and 1.6 Hz, H-6_{eq}), 0.93 (9 H, s, $C(CH_3)_3$), 0.88 (9 H, s, $C(CH_3)_3$), 0.20 (3 H, s, $SiCH_3$), 0.16 (3 H, s, $SiCH_3$), 0.09 (3 H, s, $SiCH_3$) and 0.07 (3 H, s, $SiCH_3$); δ_C (100 MHz; $CDCl_3$): 174.9 (C), 140.9 (CH), 140.6 (C), 137.9 (C), 130.1 (C), 124.5 (CH), 124.1 (CH), 123.2 (CH), 122.9 (CH), 122.6 (C), 121.3 (CH), 88.2 (C), 80.2 (C), 75.8 (CH), 74.9 (C), 68.2 (CH), 36.8 (CH_2), 25.6 (2 × C(*C*H_3)$_3$), 19.6 (CH_2), 18.0 (2 × *C*(CH_3)$_3$), −3.1 (2 × $SiCH_3$), −4.7 ($SiCH_3$) and −4.9 ($SiCH_3$); ν_{max} (KBr)/cm^{-1} 2227 (C≡C) and 1803 (CO); MS (CI) m/z = 555 (MH^+); HRMS (CI) calcd for $C_{30}H_{42}O_4SSi_2Na$ (MNa^+): 555.2408, found 555.2415.

(1*R*,4*R*,5*R*)-1,4-Di(*tert*-butyldimethylsilyloxy)-3-(3-(naphth-2-yl)propyl)cyclohex-2-en-1,5-carbolactone (25a)

The experimental procedure used was the same as for compound **15a** using alkyne **24a** (168 mg, 0.30 mmol), Rosemund's catalyst (150 mg) and 50% THF–methanol (6 mL). Purification by flash chromatography on silica gel, eluting with (30 : 70) dichloromethane–hexanes, gave saturated derivative **25a** (166 mg, 98%) as a colorless oil. $[\alpha]_{20}^{D}$ = −49.1° (*c* 1.0 in MeOH); δ_H (400 MHz; $CDCl_3$): 7.76–7.58 (3 H, m, 3 × ArH), 7.47 (1 H, br s, ArH), 7.45–7.39 (2 H, m, 2 × ArH), 7.29 (2 H, dd, J = 1.6 and 8.4 Hz, 2 × ArH), 5.73 (1 H, d, J = 1.6 Hz, H-2), 4.45 (1 H, m, H-5), 4.00 (1 H, d, J = 3.2 Hz, H-4), 2.85 (2 H, td, J = 1.6 and 7.2 Hz, CH_2Ar), 2.31 (2 H, m, CH_2), 2.06 (2 H, m, CH_2),

1.83 (2 H, m, CH_2), 0.92 (9 H, s, $C(CH_3)_3$), 0.85 (9 H, s, C $(CH_3)_3$), 0.18 (3 H, s, $SiCH_3$), 0.14 (3 H, s, $SiCH_3$), 0.09 (3 H, s, $SiCH_3$) and 0.04 (3 H, s, $SiCH_3$); δ_C (100 MHz; $CDCl_3$): 176.1 (C), 139.2 (C), 138.9 (C), 133.6 (C), 132.0 (C), 130.7 (CH), 128.0 (CH), 127.6 (CH), 127.4 (CH), 127.2 (CH), 126.5 (CH), 125.9 (CH), 125.1 (CH), 76.0 (CH), 74.7 (C), 67.7 (CH), 37.2 (CH_2), 35.6 (CH_2), 31.4 (CH_2), 28.5 (CH_2), 25.6 (2 × C $(CH_3)_3$), 18.0 ($C(CH_3)_3$), −17.8 ($C(CH_3)_3$), −3.0 (2 × $SiCH_3$), −4.6 ($SiCH_3$) and −4.8 ($SiCH_3$); ν_{max} (film)/cm^{-1} 1799 (CO); MS (ESI) m/z = 553 (MH^+); HRMS (ESI) calcd for $C_{32}H_{49}Si_2O_4$ (MH^+): 553.3164, found 553.3145.

(1*R*,4*R*,5*R*)-3-(3-(Benzo[*b*]thiophen-3-yl)propyl)-1,4-di(*tert*-butyldime-thylsilyloxy)cyclohex-2-en-1,5-carbolactone (25d)

The experimental procedure used was the same as for saturated derivative **15a** utilizing alkyne **24d** (60 mg, 0.11 mmol). Yield = 60 mg (98%). Yellow oil. $[\alpha]_{20}^{D}$ = −86.4° (*c* 1.0 in $CHCl_3$); δ_H (250 MHz; $CDCl_3$): 7.86 (1 H, d, *J* = 7.3 Hz, ArH), 7.72 (1 H, d, *J* = 8.2 Hz, ArH), 7.38 (2 H, m, 2 × ArH), 7.07 (1 H, s, ArH), 5.76 (1 H, s, H-2), 4.48 (1 H, m, H-5), 4.01 (1 H, d, *J* = 3.0 Hz, H-4), 2.85 (2 H, t, *J* = 7.3 Hz, CH_2Ar), 2.32 (2 H, m, CH_2-6), 2.12 (2 H, m, CH_2), 1.88 (2 H, m, CH_2), 0.93 (9 H, s, $C(CH_3)_3$), 0.87 (9 H, s, $C(CH_3)_3$), 0.19 (3 H, s, $SiCH_3$), 0.14 (3 H, s, $SiCH_3$), 0.10 (3 H, s, $SiCH_3$) and 0.04 (3 H, s, $SiCH_3$); δ_C (63 MHz; $CDCl_3$): 176.1 (C), 140.5 (C), 138.8 (C), 138.7 (C), 136.1 (C), 130.8 (CH), 124.1 (CH), 123.9 (CH), 122.9 (CH), 121.6 (CH), 121.4 (CH), 75.9 (CH), 74.7 (C), 67.7 (CH), 37.2 (CH_2), 31.2 (CH_2), 28.0 (CH_2), 26.6 (CH_2), 25.6 (2 × $C(CH_3)_3$), 18.0 ($C(CH_3)_3$), 17.9 ($C(CH_3)_3$), 1.0 ($SiCH_3$), −3.0 ($SiCH_3$), and −4.6 ($SiCH_3$), −4.8 ($SiCH_3$); ν_{max} (film)/cm^{-1} 1799 (CO); MS (CI) m/z = 559 (MH^+).

(1*R*,4*R*,5*R*)-1,4-Dihydroxy-3-(3-(naphth-2-yl)propyl)cyclohex-2-en-1,5-carbolactone (26a)

The experimental procedure used was the same as for diol **14a** utilizing silyl ether **25a** (38 mg, 0.07 mmol). Purification by flash chromatography on silica gel, eluting with (1 : 1 : 1) diethyl ether–acetone–hexanes, gave diol **26a** (17 mg, 77%) as a white foam. $[\alpha]_{20}^{D}$ = −151.4° (*c* 1.0 in MeOH); Mp: 125–128 °C; δ_H (400 MHz; CD_3OD): 7.71 (3 H, m, 3 × ArH), 7.53 (1 H, br s, ArH), 7.36–7.23 (3 H, m, 3 × ArH), 5.74 (1 H, s, H-2), 4.56 (1 H, m, H-5), 3.98 (1 H, d, *J* = 4.0 Hz, H-4), 2.67 (2 H, t, *J* = 7.0 Hz, CH_2Ar), 2.27 (2 H, m, CH_2-6), 2.12 (2 H, m, CH_2) and 1.81 (2 H, m, CH_2); δ_C (100 MHz; CD_3OD): 179.3 (C), 141.2 (C), 140.7 (C), 135.1 (C), 133.5 (C), 130.8 (CH), 128.9 (CH), 128.6 (CH), 128.5 (CH), 128.3 (CH), 127.5 (CH), 126.9 (CH), 126.1 (CH), 78.0 (CH), 74.0 (C), 67.6 (CH), 37.5 (CH_2), 36.3 (CH_2), 32.5 (CH_2) and 29.7 (CH_2); ν_{max} (KBr)/cm^{-1} 3431 (OH), 3290 (OH) and 1757 (CO); MS (ESI) m/z = 323 ($M - H^+$); HRMS (ESI) calcd for $C_{20}H_{19}O_4$ ($M - H^+$): 323.1278, found 323.1287.

(1*R*,4*R*,5*R*)-3-(3-(Benzo[*b*]thiophen-3-yl)propyl)-1,4-dihydroxy-cyclohex-2-en-1,5-carbolactone (26d)

The experimental procedure used was the same as for diol **14a** utilizing silyl ether **25d** (85 mg, 0.15 mmol). Yield: 33 mg (67%). White solid. Mp: 156–160 °C. $[\alpha]_{20}^{D}$ = −128.7° (*c* 1.0 in MeOH); δ_H (500 MHz; CD_3OD): 7.80 (1 H, d, *J* = 8.0 Hz, ArH), 7.70 (1 H, d, *J* = 8.0 Hz, ArH), 7.35–7.27 (2 H, m, 2 × ArH), 7.16 (1 H, s, ArH), 5.79 (1 H, s, H-2), 4.59 (1 H, m, H-5), 4.01 (1 H, d, *J* = 3.5 Hz, H-4), 2.78 (2 H, m, CH_2Ar), 2.32–2.27 (2 H, m, CH_2-6), 2.25–2.21 (2 H, m, CH_2), 1.97 (1 H, m, C*H*H) and 1.86–1.77 (1 H, m, CH*H*); δ_C (63 MHz; acetone-d_6): 178.6 (C), 141.3 (2 × C), 140.8 (C), 138.3 (C), 131.7 (CH), 126.0 (CH), 125.7 (CH), 124.5 (CH), 123.5 (CH), 123.2 (CH), 78.0 (CH), 74.6 (C), 68.4 (CH), 38.2 (CH_2), 33.4 (CH_2), 29.4 (CH_2) and 28.4 (CH_2); ν_{max} (KBr)/cm^{-1} 2952 (OH), 2929 (OH) and 1799 (CO); MS (ESI) m/z = 353 (MNa^+); HRMS (ESI) calcd for $C_{18}H_{18}O_4SNa$ (MNa^+): 353.0823, found 353.0818.

(1*R*,4*R*,5*R*)-1,4,5-Trihydroxy-3-(3-(naphth-2-yl)propyl)cyclohex-2-ene-1-carboxylic acid (7a)

The experimental procedure used was the same as for acid **5a** utilizing lactone **26a** (30 mg, 0.09 mmol). Yield = 30 mg (94%). White solid. $[\alpha]_{20}^{D}$ = −23.2° (*c* 1.0 in MeOH); Mp: 154–158 °C; δ_H (400 MHz; CD_3OD): 7.67 (3 H m, 3 × ArH), 7.54 (1 H, br s, ArH), 7.30 (3 H, m, 3 × ArH), 5.38 (1 H, s, H-2), 3.81 (2 H, m, H-5 + H-4), 2.70 (2 H, m, CH_2Ar), 2.34 (1 H, m, C*H*H) and 2.06–1.75 (5 H, m, CH*H*+2 × CH_2); ^{13}C NMR (100 MHz, CD_3OD) δ: 178.4 (C), 145.1 (C), 141.1 (C), 135.2 (C), 133.5 (C), 128.8 (CH), 128.6 (CH), 128.4 (2 × CH), 127.6 (CH), 126.8 (CH), 126.1 (CH), 124.9 (CH), 74.7 (CH), 74.3 (C), 71.1 (CH), 40.5 (CH_2), 36.3 (CH_2), 33.1 (CH_2) and 30.1 (CH_2); ν_{max} (KBr)/cm^{-1} 3390 (OH) and 1718 (CO) cm^{-1}. MS (ESI) m/z = 341 [M − H]; HRMS (ESI) calcd for $C_{20}H_{21}O_5$ [M − H]: 341.1384, found 341.1384.

(1*R*,4*R*,5*R*)-3-(3-(Benzo[*b*]thiophen-3-yl)propyl)-1,4,5-trihydroxycyclohex-2-ene-1-carboxylic acid (7d)

The experimental procedure used was the same as for acid **5a** utilizing diol **26d** (30 mg, 0.09 mmol). Yield = 26 mg (87%). White solid. Mp: 118–119 °C. $[\alpha]_{20}^{D}$ = −34.1° (*c* 1.0, MeOH). ^{1}H NMR (400 MHz, CD_3OD) δ: 7.82 (1 H, d, *J* = 8.0 Hz, ArH), 7.77 (1 H, d, *J* = 7.2 Hz, ArH), 7.36–7.27 (2 H, m, 2 × ArH), 7.21 (1 H, s, ArH), 5.47 (1 H, s, H-2), 3.91–3.84 (2 H, m, H-5 + H-4), 2.95–2.79 (2 H, m, CH_2), 2.54–2.42 (1 H, m, C*H*H) and 2.18–1.80 (5 H, m, 2 × CH_2 + CH*H*); δ_C (100 MHz; CD_3OD): 178.8 (C), 144.7 (C), 141.9 (C), 140.4 (C), 137.9 (C), 125.3 (CH), 125.2 (CH), 124.9 (CH), 123.7 (CH), 122.8 (CH), 122.4 (CH), 74.6 (CH), 74.4 (C), 71.1 (CH), 40.3 (CH_2), 33.4 (CH_2), 28.8 (CH_2) and 28.2 (CH_2); ν_{max} (KBr)/cm^{-1} 3367 (OH) and 1709 (CO); MS (ESI) m/z = 347 ($M - H^+$); HRMS (ESI) calcd for $C_{18}H_{19}O_5S$ ($M - H^+$): 347.0948, found 347.0955.

Preparation of 25a by *B*-alkyl Suzuki cross-coupling

(a) Preparation of borane 23a. To a solution of 9-BBN-H (0.4 mL, 0.20 mmol, *ca.* 0.5 M in THF) in a flamed round-bottom flask under argon 2-allylnaphthalene (**22a**) (63 mg, 0.37 mmol) was added. The mixture was stirred for 12 h to give a solution of borane **23a**.

(b) *B*-alkyl Suzuki cross-coupling. To the borane solution obtained above, K_3PO_4 (63 mg, 0.28 mmol), $Pd(PPh_3)_4$ (33 mg, 0.03 mmol), dioxane (0.8 mL) and triflate **12**[2c] (100 mg, 0.12 mmol) were added. The resultant solution was heated at 110 °C for 12 h under argon. After cooling to room temperature, the solution was diluted with diethyl ether and water. The organic layer was separated and the aqueous phase was extracted with diethyl ether (×2). The combined organic extracts were dried (Na_2SO_4), filtered and concentrated under reduced pressure. The residue was purified by flash chromatography on silica gel, eluting with a gradient of dichloromethane–hexanes (10 : 90 to 40 : 60), to give compound **25a** (73 mg, 70%).

Preparation of 25d by *B*-alkyl Suzuki cross-coupling

(a) Preparation of borane 23d. To a solution of 9-BBN-H (0.44 mL, 0.22 mmol, *ca.* 0.5 M in THF) in a flamed round-bottom flask under argon 3-allylbenzo[*b*]thiophene (**22d**) (65 mg, 0.37 mmol) was added. The mixture was stirred for 12 h to give a solution of borane **23d**.

(b) B-alkyl Suzuki cross-coupling. To the borane solution obtained above, K_3PO_4 (84 mg, 0.38 mmol), $Pd(PPh_3)_4$ (32 mg, 0.03 mmol), dioxane (0.8 mL), KBr (25 mg, 0.21 mmol) and triflate **12**[2c] (100 mg, 0.12 mmol) were added. The resultant solution was heated at 110 °C for 12 h under argon. After cooling to room temperature, the solution was diluted with diethyl ether and water. The organic layer was separated and the aqueous phase was extracted with diethyl ether (×2). The combined organic extracts were dried (Na_2SO_4), filtered and concentrated under reduced pressure. The residue was purified by flash chromatography on silica gel, eluting with a gradient of dichloromethane–hexanes (10 : 90 to 40 : 60), to give compound **25d** (44 mg, 42%).

Dehydroquinase assays

The enzyme was purified and assayed as described previously.[2d,12]

Docking studies

They were carried out using the program GOLD 5.0.1[9] and the enzyme geometries found in the crystal structure of the binary complex DHQ2-Hp/**4c** (PDB code: 2WKS[5a]) and DHQ2-Mt/**4c** (PDB code: 2Y71[5b]) In the latter case, not solved residues 18–20 were incorporated from the crystal structure of the fully resolved crystal structure of DHQ2-Mt in complex with (1*R*,2*R*,4*S*,5*R*)-1,4,5-trihydroxy-2-(4-methoxybenzyl)-3-oxocyclohexanecarboxylic acid (PDB code: 2XB8[7]) The receptor was used as a dimer. Water molecules were removed from all crystal structures with the exception of the water involved in the mechanism, which is located close to the carbonyl group of C3. Ligand geometries were minimized using the AM1 Hamiltonian as implemented in the program Gaussian 09[13] and used as MOL2 files. Each ligand was docked in 25 independent genetic algorithm (GA) runs, and for each of these a maximum number of 100 000 GA operations were performed on a single population of 50 individuals. Operator weights for crossover, mutation and migration in the entry box were used as default parameters (95, 95, and 10, respectively), as well as the hydrogen bonding (4.0 Å) and van der Waals (2.5 Å) parameters. The position of ligand **4c** in both crystal structures was used to define the active-site and the radius was set to 7 Å. The "flip ring corners" flag was switched on, while all the other flags were off. The GOLD scoring function was used to rank the ligands in order of fitness.

Molecular dynamics simulations

Ligand minimization. Ligand geometries were first refined by means of the semi-empirical quantum mechanical program MOPAC[14] using the AM1 Hamiltonian and PRECISE stopping criteria, and further optimised using a restricted Hartree–Fock (RHF) method and a 6-31G(d) basis set, as implemented in the *ab initio* program Gaussian 09.[13] The resulting wavefunctions were used to calculate electrostatic potential-derived (ESP) charges employing the restrained electrostatic potential (RESP)[15] methodology, as implemented in the assisted model building with energy refinement (AMBER)[16] suite of programs. The missing bonded and non-bonded parameters were assigned, by analogy or through interpolation from those already present in the AMBER database (GAFF).[13,17]

Generation and minimization of the DHQ2–ligand complexes. Simulations were carried out using the enzyme geometries found in the crystal structure of DHQ2-Mt in complex **4c** (PDB code 2Y71[5b]). Not solved residues 18–20 were incorporated from the crystal structure of the fully resolved crystal structure of DHQ2-Mt in complex with (1*R*,2*R*,4*S*,5*R*)-1,4,5-trihydroxy-2-(4-methoxybenzyl)-3-oxocyclohexanecarboxylic acid (PDB code: 2XB8[7]). Taking into account that unfolding and refolding studies of DHQ2 have shown that the trimer[18] is the biological unit of the enzyme and on the basis of preliminary simulations on the monomer proving to be unstable under our simulation conditions, the trimer was used for these studies. Hydrogens were added to the protein using the web-based PROPKA3.1 server,[19] which assigned protonation states to all titratable residues at the chosen pH of 7.0. However, δ and/or ε protonation was manually corrected for His102 (dual) of the active site due to the mechanistic considerations and on the basis of results from preliminary MD simulations. Molecular mechanics parameters from the ff03 and GAFF force fields, respectively, were assigned to the protein and the ligands using the LEaP module of AMBER 10.0.[20] All terminal hydrogens were first minimized *in vacuo* (2000 steps, half of them steepest descent, the other half conjugate gradient). Then, energy minimization using the implicit solvent GB model was carried out in stages, starting with ligand (1000 steps, half of them steepest descent, the other half conjugate gradient), protein side-chains (1000 steps, *idem*) and finally the entire complex (1000 steps, *idem*). A positional *restraint* force constant of 50 kcal mol^{-1} $Å^{-2}$ to those unminimized atoms in each step was applied during all calculations. Thereafter each refined DHQ2–ligand complex was neutralized by addition of sodium ions and immersed in a truncated octahedron of TIP3P water molecules.[16,21,22]

Simulations. MD simulations were performed using the AMBER 10.0 suite of programs and Amber ff03 force field.

Periodic boundary conditions were applied and electrostatic interactions were treated using the smooth particle mesh Ewald method (PME)[23] with a grid spacing of 1 Å. The cutoff distance for the non-bonded interactions was 9 Å. SHAKE algorithm[24] was applied to all bonds containing hydrogen, using a tolerance of 10^{-5} Å and an integration step of 2.0 fs. Minimization was carried out in three steps, starting with the octahedron water hydrogens, followed by solvent molecules and sodium counterions and finally the entire system. The minimized system was heated at 300 K (1 atm, 25 ps, a positional *restraint* force constant of 50 kcal mol^{-1} $Å^{-2}$). These initial harmonic restraints were gradually reduced to 5 kcal mol^{-1} $Å^{-2}$ (10 steps) and the resulting systems were allowed to equilibrate further. MD with constraints of 5 kcal mol^{-1} $Å^{-2}$ were carried out to all protein α-carbons of the two external subunits of the trimer and the beta sheets and alpha helix of the central subunit of the trimer for 10 ns (500 steps). System coordinates were collected every 2 ps for further analysis. Next, a slow-cooling MD simulation with constraints of 5 kcal mol^{-1} $Å^{-2}$ was performed (6 steps until 273 K). Finally, minimization of the entire complexes was performed with constraints of 5 kcal mol^{-1} $Å^{-2}$.

Acknowledgements

Financial support from the Xunta de Galicia (10PXIB2200122PR and GRC2010/12) and the Spanish Ministry of Science and Innovation (SAF2010-15076) is gratefully acknowledged. BB, AS and AP thank the Spanish Ministry of Science and Innovation for FPU fellowships. We are also grateful to the Centro de Supercomputación de Galicia (CESGA) for the use of the Finis Terrae computer.

Notes and references

1 A. Koul, E. Arnoult, N. Lounis, J. Guillemont and K. Andries, *Nature*, 2011, **469**, 489–490.
2 (*a*) C. González-Bello and L. Castedo, *Med. Res. Rev.*, 2007, **27**, 177–208; (*b*) C. González-Bello, E. Lence, M. D. Toscano, L. Castedo, J. R. Coggins and C. Abell, *J. Med. Chem.*, 2003, **46**, 5735–5744; (*c*) C. Sánchez-Sixto, V. F. V. Prazeres, L. Castedo, H. Lamb, A. R. Hawkins and C. González-Bello, *J. Med. Chem.*, 2005, **48**, 4871–4881; (*d*) V. F. V. Prazeres, C. Sánchez-Sixto, L. Castedo, H. Lamb, A. R. Hawkins, A. Riboldi-Tunnicliffe, J. R. Coggins, A. J. Lapthorn and C. González-Bello, *ChemMedChem*, 2007, **2**, 194–207; (*e*) C. Sánchez-Sixto, V. F. V. Prazeres, L. Castedo, S. W. Suh, H. Lamb, A. R. Hawkins, F. J. Cañada, J. Jiménez-Barbero and C. González-Bello, *ChemMedChem*, 2008, **3**, 756–770.
3 See also: (*a*) M. Frederickson, E. J. Parker, A. R. Hawkins, J. R. Coggins and C. Abell, *J. Org. Chem.*, 1999, **64**, 2612–2613; (*b*) M. Frederickson, A. W. Roszak, J. R. Coggins, A. J. Lapthorn and C. Abell, *Org. Biomol. Chem.*, 2004, **2**, 1592–1596; (*c*) M. D. Toscano, R. J. Payne, A. Chiba, O. Kerbarh and C. Abell, *ChemMedChem*, 2007, **2**, 101–112; (*d*) R. J. Payne, F. Peyrot, O. Kerbarh, A. D. Abell and C. Abell, *ChemMedChem*, 2007, **2**, 1015–1029; (*e*) R. J. Payne, A. Riboldi-Tunnicliffe, O. Kerbarh, A. D. Abell, A. J. Lapthorn and C. Abell, *ChemMedChem*, 2007, **2**, 1010–1013; (*f*) A. T. Tran, K. M. Cergol, N. P. West, E. J. Randall, W. J. Britton, S. A. I. Bokhari, M. Ibrahim, A. J. Lapthorn and R. J. Payne, *ChemMedChem*, 2011, **6**, 262–265; (*g*) M. V. B. Dias, W. C. Snee, K. M. Bromfield, E. J. Payne, S. K. Palaninathan, A. Ciulli, N. I. Howard, C. Abell, J. C. Sacchettini and T. L. Blundell, *Biochem. J.*, 2011, **436**, 729–739.
4 (*a*) J. Harris, C. González-Bello, C. Kleanthous, J. R. Coggins, A. R. Hawkins and C. Abell, *Biochem. J.*, 1996, **319**, 333–336; (*b*) A. W. Roszak, D. A. Robinson, T. Krell, I. S. Hunter, M. Frederickson, C. Abell, J. R. Coggins and A. J. Lapthorn, *Structure*, 2002, **10**, 493–503.
5 (*a*) V. F. V. Prazeres, L. Tizón, J. M. Otero, P. Guardado-Calvo, A. L. Llamas-Saíz, M. J. van Raaij, L. Castedo, H. Lamb, A. R. Hawkins and C. González-Bello, *J. Med. Chem.*, 2010, **53**, 191–200; (*b*) L. Tizón, J. M. Otero, V. F. V. Prazeres, A. L. Llamas-Saíz, M. J. van Raaij, H. Lamb, A. R. Hawkins, J. A. Ainsa, L. Castedo and C. González-Bello, *J. Med. Chem.*, 2011, **54**, 6063–6084.
6 This figure was prepared using PyMOL: W. L. DeLano, *The PyMOL Molecular Graphics System*, DeLano Scientific LLC, Palo Alto, CA, USA, 2008. http://www.pymol.org
7 A. Peón, J. M. Otero, L. Tizón, V. F. V. Prazeres, A. L. Llamas-Saiz, G. C. Fox, M. J. van Raaij, H. Lamb, A. R. Hawkins, F. Gago, L. Castedo and C. González-Bello, *ChemMedChem*, 2010, **5**, 1726–1733.
8 S. R. Chemler, D. Trauner and S. J. Danishefsky, *Angew. Chem., Int. Ed.*, 2001, **40**, 4544–4568; S. R. Chemler, D. Trauner and S. J. Danishefsky, *Angew. Chem.*, 2001, **113**, 4676–4701.
9 http://www.ccdc.cam.ac.uk/products/life_sciencies/gold/
10 J. Fournier dit Chabert, B. Márquez, L. Neville, L. Joucla, S. Broussous, P. Bouhours, E. David, S. Pellet-Rostaing, B. Marquet, N. Moreau and M. Lemaire, *Bioorg. Med. Chem.*, 2007, **15**, 4482–4497.
11 C. S. Bryan, J. A. Braunger and M. Lautens, *Angew. Chem., Int. Ed.*, 2009, **48**, 7064–7068; C. S. Bryan, J. A. Braunger and M. Lautens, *Angew. Chem.*, 2009, **121**, 7198–7202.
12 D. G. Gourley, J. R. Coggins, N. W. Isaacs, J. D. Moore, I. G. Charles and A. R. Hawkins, *J. Mol. Biol.*, 1994, **241**, 488–491.
13 M. J. Frisch, G. W. Trucks, H. B. Schlegel, G. E. Scuseria, M. A. Robb, J. R. Cheeseman, G. Scalmani, V. Barone, B. Mennucci, G. A. Petersson, H. Nakatsuji, M. Caricato, X. Li, H. P. Hratchian, A. F. Izmaylov, J. Bloino, G. Zheng, J. L. Sonnenberg, M. Hada, M. Ehara, K. Toyota, R. Fukuda, J. Hasegawa, M. Ishida, T. Nakajima, Y. Honda, O. Kitao, H. Nakai, T. Vreven, J. A. Montgomery Jr., J. E. Peralta, F. Ogliaro, M. Bearpark, J. J. Heyd, E. Brothers, K. N. Kudin, V. N. Staroverov, R. Kobayashi, J. Normand, K. Raghavachari, A. Rendell, J. C. Burant, S. S. Iyengar, J. Tomasi, M. Cossi, N. Rega, J. M. Millam, M. Klene, J. E. Knox, J. B. Cross, V. Bakken, C. Adamo, J. Jaramillo, R. Gomperts, R. E. Stratmann, O. Yazyev, A. J. Austin, R. Cammi, C. Pomelli, J. W. Ochterski, R. L. Martin, K. Morokuma, V. G. Zakrzewski, G. A. Voth, P. Salvador, J. J. Dannenberg, S. Dapprich, A. D. Daniels, Ö. Farkas, J. B. Foresman, J. V. Ortiz, J. Cioslowski and D. J. Fox, *GAUSSIAN 09 (Revision A.2)*, Gaussian, Inc., Wallingford CT, 2009.
14 J. Stewart, *J. Comput.-Aided Mol. Des.*, 1990, **4**, 1–45.
15 (*a*) W. D. Cornell, P. Cieplak, C. I. Bayly, I. R. Gould, K. M. Merz, D. M. Ferguson, D. C. Spellmeyer, T. Fox, J. W. Caldwell and P. A. Kollman, *J. Am. Chem. Soc.*, 1995, **117**, 5179–5197; (*b*) http://q4md-forcedfieldtools.org/RED/resp/
16 D. A. Case, T. E. Cheatham, T. Darden, H. Gohlke, R. Luo, K. M. Merz, O. Onufriev, C. Simmerling, B. Wang and R. J. Woods, *J. Comput. Chem.*, 2005, **26**, 1668–1688.
17 (*a*) J. Wang, R. M. Wolf, J. W. Caldwell, P. A. Kollman and D. A. Case, *J. Comput. Chem.*, 2004, **25**, 1157–1174; (*b*) J. Wang, W. Wang, P. A. Kollman and D. A. Case, *J. Mol. Graphics Modell.*, 2006, **25**, 247–260.
18 N. C. Price, D. J. Boam, S. M. Kelly, D. Duncan, T. Krell, D. G. Gourley, J. R. Coggins, R. Virden and A. R. Hawkins, *Biochem. J.*, 1999, **338**, 195–202.
19 (*a*) H. Li, A. D. Robertson and J. H. Jensen, *Proteins: Struct., Funct., Bioinf.*, 2005, **61**, 704–721; (*b*) D. C. Bas, D. M. Rogers and J. H. Jensen, *Proteins: Struct., Funct., Bioinf.*, 2008, **73**, 765–783; (*c*) M. H. M. Olsson, C. R. Søndergard, M. Rostkowski and J. H. Jensen, *J. Chem. Theory Comput.*, 2011, **7**, 525–537; (*d*) C. R. Søndergard, M. H. M. Olsson, M. Rostkowski and J. H. Jensen, *J. Chem. Theory Comput.*, 2011, **7**, 2284–2295.
20 D. A. Case, T. A. Darden, T. E. Cheatham III, C. L. Simmerling, J. Wang, R. E. Duke, R. Luo, R. C. Walker, W. Zhang, K. M. Merz, B. Roberts, B. Wang, S. Hayik, A. Roitberg, G. Seabra, I. Kolossvai, K. F. Wong, F. Paesani, J. Vanicek, J. Liu, X. Wu, S. R. Brozell, T. Steinbrecher, H. Gohlke, Q. Cai, X. Ye, J. Wang, M.-J. Hsieh, G. Cui, D. R. Roe, D. H. Mathews, M. G. Seetin, C. Sagui, V. Babin, T. Luchko, S. Gusarov, A. Kovalenko and P. A. Kollman, *Amber Tools 1.5, AMBER 11*, University of California, San Francisco, 2010.
21 J. Aqvist, *J. Phys. Chem.*, 1990, **94**, 8021–8024.
22 W. L. Jorgensen, J. Chandrasekhar and J. D. Madura, *J. Chem. Phys.*, 1983, **79**, 926–935.
23 T. A. Darden, D. York and L. G. Pedersen, *J. Chem. Phys.*, 1993, **98**, 10089–10092.
24 J.-P. Ryckaert, G. Ciccotti and H. J. C. Berendsen, *J. Comput. Phys.*, 1977, **23**, 327–341.

